paradigms (Raichle et al., 1994; Poldrack et al., 1998; Poldrack and Gabrieli, 2001). Whereas the good spatial replicability demonstrated in the present study in contrast to these previous findings may be attributed to several heterogeneous scanning conditions, it would be difficult to detect similar activation region alternation in NIRS examinations which measure not a whole brain but only surface regions of certain parts of the cerebral cortices, even if such alternation actually occurs. However, the current finding of small spatial variation within the inherent spatial resolution of NIRS in spite of repeated optode repositioning suggest sufficient spatial replicability for actual NIRS measurements in relevant cortical regions during cognitive activations.

The temporal replicability in terms of correlation coefficients between [Hb] change time courses was acceptable. However, it was inferior to that in the above-mentioned report by Sato et al. (2006) which demonstrated mean correlation coefficients around 0.85. Whereas data processing are heterogeneous between the present study and theirs on some points (they selected variable time windows from a certain extent and variable single channels allowing disagreement between sessions, both of which were of the largest absolute magnitude of [Hb] change), the current difference may be caused by the major difference in the nature of the relevant activation tasks: demand for active performance in cognitive tasks in contrast to the passiveness in sensory tasks.

There were some methodological limitations in the present study. First, the sample size was small. As far as considering the mean values of [oxyHb] change, we observed a tendency of decrease in the 3rd and 4th sessions as compared with the 1st and 2nd, though it did not reach statistical significance. It should be confirmed by examining a larger number of subjects, and using various types of cognitive activation tasks. Secondly, we examined only men, failing to examine sex differences. Women should also be included in future studies. In women, however, cognitive function may vary with menstrual cycle (Postma et al., 1999; Dietrich et al., 2001; Hausmann et al., 2002; Maki et al., 2002; Rosenberg and Park, 2002). Thus, the effects of menstrual cycle should be considered when women are included in studies.

In conclusion, the current findings suggest a considerable replicability for multiple-time measurements of prefrontal [oxyHb] and [deoxyHb] changes during cognitive activation in men. Further studies addressing various measurement conditions such as measurement interval, times of repetition and kind of activation task are necessary to identify better measurement methodologies with stable multiple-time replicability. At the same time, the sensitivity of NIRS signals to longitudinal changes in cerebral function following certain interventions (e.g., pharmacological or cognitive–behavioral interventions) should be investigated. Coupled with such evidence, our observations might provide support for clinical utility of NIRS in the field of neuropsychiatry.

Acknowledgements

This study was supported in part by Grant-in-Aid for Scientific Research on Priority Areas-Research on Pathomechanisms of Brain Disorders from the Ministry of Education, Culture, Sports, Science and Technology of Japan (No. 17025015 to K.K.), and The Japan Society for Promotion of Science (No. P05234 to M.R.). We thank Ms. Keiko Tanaka for recruiting subjects and helping to coordinate their schedules of experiment.

References

Audenaert, K., Brans, B., Van Laere, K., Lahorte, P., Versijpt, J., van Heeringen, K., Dierckx, R., 2000. Verbal fluency as a prefrontal activation probe: a validation study using ^{99}mTc-ECD brain SPET. Eur. J. Nucl. Med. 27, 1800–1808.

Claassen, J.A., Colier, W.N., Jansen, R.W., 2006. Reproducibility of cerebral blood volume measurements by near infrared spectroscopy in 16 healthy elderly subjects. Physiol. Meas. 27, 255–264.

Cohen, J., 1977. Statistical Power Analysis for the Behavioral Sciences, revised ed. Academic Press, New York, p. 40.

Dietrich, T., Krings, T., Neulen, J., Willmes, K., Erberich, S., Thron, A., Sturm, W., 2001. Effects of blood estrogen level on cortical activation patterns during cognitive activation as measured by functional MRI. NeuroImage 13, 425–432.

Fallgatter, A.J., Strik, W.K., 1997. Right frontal activation during the continuous performance test assessed with near-infrared spectroscopy in healthy subjects. Neurosci. Lett. 223, 89–92.

Fallgatter, A.J., Strik, W.K., 1998. Frontal brain activation during the Wisconsin Card Sorting Test assessed with two-channel near-infrared spectroscopy. Eur. Arch. Psychiatry Clin. Neurosci. 248, 245–249.

Fallgatter, A.J., Strik, W.K., 2000. Reduced frontal functional asymmetry in schizophrenia during a cued continuous performance test assessed with near-infrared spectroscopy. Schizophr. Bull. 26, 913–919.

Gratton, G., Maier, J.S., Fabiani, M., Mantulin, W.W., Gratton, E., 1994. Feasibility of intracranial near-infrared optical scanning. Psychopsysiology 31, 211–215.

Harrington, G.S., Buonocore, M.H., Farias, S.T., 2006. Intrasubject reproducibility of functional MR imaging activation in language tasks. Am. J. Neuroradiol. 27, 938–944.

Hausmann, M., Becker, C., Gather, U., Gunturkun, O., 2002. Functional cerebral asymmetries during the menstrual cycle: a cross-sectional and longitudinal analysis. Neuropsychologia 40, 808–816.

Hempel, A., Giesel, F.L., Garcia Caraballo, N.M., Amann, M., Meyer, H., Wustenberg, T., Essig, M., Schroder, J., 2004. Plasticity of cortical activation related to working memory during training. Am. J. Psychiatry 161, 745–747.

Herrmann, M.J., Ehlis, A.C., Fallgatter, A.J., 2004. Bilaterally reduced frontal activation during a verbal fluency task in depressed patients as measured by near-infrared spectroscopy. J. Neuropsychiatry Clin. Neurosci. 16, 170–175.

Hock, C., Muller-Spahn, F., Schuh-Hofer, S., Hofmann, M., Dirnagl, U., Villringer, A., 1995. Age dependency of changes in cerebral hemoglobin oxygenation during brain activation: a near-infrared spectroscopy study. J. Cereb. Blood Flow Metab. 15, 1103–1108.

Hock, C., Villinger, K., Muller-Spahn, F., Wenzel, R., Heekeren, H., Schuh-Hofer, S., Hofmann, M., Minoshima, S., Schwaiger, M., Dirnagl, U., Villringer, A., 1997. Decrease in parietal cerebral hemoglobin oxygenation during performance of a verbal fluency task in patients with Alzheimer's disease monitored by means of near-infrared spectroscopy (NIRS)—correlation with simultaneous rCBF-PET measurements. Brain Res. 755, 293–303.

Honda, M., Deiber, M.P., Ibanez, V., Pascual-Leone, A., Zhuang, P., Hallett, M., 1998. Dynamic cortical involvement in implicit and explicit motor sequence learning. A PET study. Brain 121, 2159–2173.

Hoshi, Y., Oda, I., Wada, Y., Ito, Y., Yamashita, Y., Oda, M., Ohta, K., Yamada, Y., Tamura, M., 2000. Visuospatial imagery is a fruitful strategy for the digit span backward task: a study with near-infrared optical tomography. Brain Res. Cogn. Brain Res. 9, 339–342.

Hoshi, Y., Tamura, M., 1993. Dynamic multichannel near-infrared optical imaging of human brain activity. J. Appl. Physiol. 75, 1842–1846.

Huppert, T.J., Hoge, R.D., Diamond, S.G., Franceschini, M.A., Boas, D.A., 2006. A temporal comparison of BOLD, ASL, and NIRS hemodynamic responses to motor stimuli in adult humans. NeuroImage 15, 368–382.

Jansma, J.M., Ramsey, N.F., Slagter, H.A., Kahn, R.S., 2001. Functional anatomical correlates of controlled and automatic processing. J. Cogn. Neurosci. 13, 730–743.

Jobsis, F.F., 1977. Noninvasive, infrared monitoring of cerebral and myocardial oxygen sufficiency and circulatory parameters. Science 198, 1264–1267.

Karni, A., Meyer, G., Jezzard, P., Adams, M.M., Turner, R., Ungerleider, L.G., 1995. Functional MRI evidence for adult motor cortex plasticity during motor skill learning. Nature 377, 155–158.

Langenecker, S.A., Nielson, K.A., 2003. Frontal recruitment during response inhibition in older adults replicated with fMRI. NeuroImage 20, 1384–1392.

Maki, P.M., Rich, J.B., Rosenbaum, R.S., 2002. Implicit memory varies across the menstrual cycle: estrogen effects in young women. Neuropsychologia 40, 518–529.

Matsuo, K., Kato, N., Kato, T., 2002. Decreased cerebral haemodynamic response to cognitive and physiological tasks in mood disorders as shown by near-infrared spectroscopy. Psychol. Med. 32, 1029–1037.

Matsuo, K., Kato, T., Fukuda, M., Kato, N., 2000. Alteration of hemoglobin oxygenation in the frontal region in elderly depressed patients as measured by near-infrared spectroscopy. J. Neuropsychiatry Clin. Neurosci. 12, 465–471.

Matsuo, K., Watanabe, A., Onodera, Y., Kato, N., Kato, T., 2004. Prefrontal hemodynamic response to verbal-fluency task and hyperventilation in bipolar disorder measured by multi-channel near-infrared spectroscopy. J. Affect. Disord. 82, 85–92.

Miki, A., Raz, J., van Erp, T.G., Liu, C.S., Haselgrove, J.C., Liu, G.T., 2000. Reproducibility of visual activation in functional MR imaging and effects of postprocessing. Am. J. Neuroradiol. 21, 910–915.

Miyai, I., Tanabe, H.C., Sase, I., Eda, H., Oda, I., Konishi, I., Tsunazawa, Y., Suzuki, T., Yanagida, T., Kubota, K., 2001. Cortical mapping of gait in humans: a near-infrared spectroscopic topography study. NeuroImage 14, 1186–1192.

Obrig, H., Wenzel, R., Kohl, M., Horst, S., Wobst, P., Steinbrink, J., Thomas, F., Villringer, A., 2000. Near-infrared spectroscopy: does it function in functional activation studies of the adult brain? Int. J. Psychophysiol. 35, 125–142.

Okada, F., Takahashi, N., Tokumitsu, Y., 1996. Dominance of the 'nondominant' hemisphere in depression. J. Affect. Disord. 37, 13–21.

Okada, F., Tokumitsu, Y., Hoshi, Y., Tamura, M., 1994. Impaired interhemispheric integration in brain oxygenation and hemodynamics in schizophrenia. Eur. Arch. Psychiatry Clin. Neurosci. 244, 17–25.

Oldfield, R.C., 1971. The assessment and analysis of handedness: the Edinburgh inventory. Neuropsychologia 9, 97–113.

Plichta, M.M., Herrmann, M.J., Baehne, C.G., Ehlis, A.C., Richter, M.M., Pauli, P., Fallgatter, A.J., 2006. Event-related functional near-infrared spectroscopy (fNIRS): are the measurements reliable? NeuroImage 31, 116–124.

Poldrack, R.A., Desmond, J.E., Glover, G.H., Gabrieli, J.D., 1998. The neural basis of visual skill learning: an fMRI study of mirror reading. Cereb. Cortex 8, 1–10.

Poldrack, R.A., Gabrieli, J.D., 2001. Characterizing the neural mechanisms of skill learning and repetition priming: evidence from mirror reading. Brain 124, 67–82.

Postma, A., Winkel, J., Tuiten, A., van Honk, J., 1999. Sex differences and menstrual cycle effects in human spatial memory. Psychoneuroendocrinology 24, 175–192.

Raichle, M.E., Fiez, J.A., Videen, T.O., MacLeod, A.M., Pardo, J.V., Fox, P.T., Petersen, S.E., 1994. Practice-related changes in human brain functional anatomy during nonmotor learning. Cereb. Cortex 4, 8–26.

Rombouts, S.A., Barkhof, F., Hoogenraad, F.G., Sprenger, M., Valk, J., Scheltens, P., 1997. Test–retest analysis with functional MR of the activated area in the human visual cortex. Am. J. Neuroradiol. 18, 1317–1322.

Rosenberg, L., Park, S., 2002. Verbal and spatial functions across the menstrual cycle in healthy young women. Psychoneuroendocrinology 27, 835–841.

Sato, H., Kiguchi, M., Maki, A., Fuchino, Y., Obata, A., Yoro, T., Koizumi, H., 2006. Within-subject reproducibility of near-infrared spectroscopy signals in sensorimotor activation after 6 months. J. Biomed. Opt. 11, 014021.

Sheehan, D.V., Lecrubier, Y., Sheehan, K.H., Amorim, P., Janavs, J., Weiller, E., Hergueta, T., Baker, R., Dunbar, G.C., 1998. The Mini-International Neuropsychiatric Interview (M.I.N.I.): the development and validation of a structured diagnostic psychiatric interview for DSM-IV and ICD-10. J. Clin. Psychiatry 59 (Suppl. 20), 22–33.

Singh, A.K., Dan, I., 2006. Exploring the false discovery rate in multichannel NIRS. NeuroImage 33, 542–549.

Strangman, G., Culver, J.P., Thompson, J.H., Boas, D.A., 2002. A quantitative comparison of simultaneous BOLD fMRI and NIRS recordings during functional brain activation. NeuroImage 17, 719–731.

Van de Ven, M.J., Colier, W.N., van der Sluijs, M.C., Walraven, D., Oeseburg, B., Folgering, H., 2001. Can cerebral blood volume be measured reproducibly with an improved near infrared spectroscopy system? J. Cereb. Blood Flow Metab. 21, 110–113.

Villringer, K., Minoshima, S., Hock, C., Obrig, H., Ziegler, S., Dirnagl, U., Schwaiger, M., Villringer, A., 1997. Assessment of local brain activation. A simultaneous PET and near-infrared spectroscopy study. Adv. Exp. Med. Biol. 413, 149–153.

Villringer, A., Planck, J., Hock, C., Schleinkofer, L., Dirnagl, U., 1993. Near infrared spectroscopy (NIRS): a new tool to study hemodynamic changes during activation of brain function in human adults. Neurosci. Lett. 154, 101–104.

Watanabe, A., Matsuo, K., Kato, N., Kato, T., 2003. Cerebrovascular response to cognitive tasks and hyperventilation measured by multi-channel near-infrared spectroscopy. J. Neuropsychiatry Clin. Neurosci. 15, 442–449.

Wei, X., Yoo, S.S., Dickey, C.C., Zou, K.H., Guttmann, C.R., Panych, L.P., 2004. Functional MRI of auditory verbal working memory: long-term reproducibility analysis. NeuroImage 21, 1000–1008.

Wyatt, J.S., Cope, M., Deply, D.T., Wray, S., Reynolds, E.O., 1986. Quantification of cerebral oxygenation and haemodynamics in sick newborn infants by near infrared spectrophotometry. Lancet 2, 1063–1066.

Journal of Neuroscience Research 85:479–487 (2007)

Enhanced Autophagic Cell Death in Expanded Polyhistidine Variants of HOXA1 Reduces PBX1-Coupled Transcriptional Activity and Inhibits Neuronal Differentiation

Rubigilda C. Paraguison,[1] Katsumi Higaki,[1] Kenji Yamamoto,[2] Hideo Matsumoto,[2] Tsukasa Sasaki,[3] Nobumasa Kato,[3] and Eiji Nanba[1]*

[1]Division of Functional Genomics, Research Center for Bioscience and Technology, Tottori University, Yonago, Japan
[2]Department of Psychiatry and Behavioral Sciences, Tokai University School of Medicine, Kanagawa, Japan
[3]Department of Psychiatry, Graduate School of Medicine, University of Tokyo, Tokyo, Japan

HOXA1 is a member of the homeobox gene family and is involved in early brain development. In our previous study, we identified novel variants of polyhistidine repeat tract in HOXA1 gene and showed that ectopic expression of expanded variants led to enhanced intranuclear aggregation and accelerated cell death in a time-dependent manner. Here, we further investigate the implications of polyhistidine variants on HOXA1 function. Aside from intranuclear aggregation, we observed cytosolic aggregates during the early stages of expression. Rapamycin, an autophagy inducer, resulted in decreased protein aggregation and cell death. Here, we also show an interaction between variants of HOXA1 and one of the HOX protein known cofactors, PBX1. Expanded HOXA1 variants exhibited reduced PBX1-coupled transcriptional activity through a regulatory enhancer of HOXB1. Moreover, we demonstrate that both deleted and expanded variants inhibited neurite outgrowth in retinoic acid-induced neuronal differentiation in neuroblastoma cells. These results provide further evidence that expanded polyhistidine repeats in HOXA1 enhance aggregation and cell death, resulting in impaired neuronal differentiation and cooperative binding with PBX1.

Key words: HOXA1; neuronal differentiation; PBX1; polyhistidine; protein aggregation; autophagy

HOX genes form a subset of the family of homeobox genes (Pearson et al., 2005). They are involved in specifying positional identity along the anterior-posterior axis of all bilaterian animals. In humans, the HOXA–D clusters comprise 39 HOX genes, located on chromosome regions 7p15, 17p21, 12q13, and 2q31 (Grier et al., 2005). During embryonic development, HOX genes are expressed sequentially 3′ to 5′ along the anterior to posterior axis. HOX genes contain a 61-amino-acid helix-turn-helix DNA-binding domain known as the *homeodomain* (Gehring et al., 1994). It is well established that HOX/DNA binding specificity is modified by other DNA-binding proteins, which act as cofactors. Among these are the PBX proteins, which are widely expressed in fetal and adult tissues and interact preferentially with 3′ HOX proteins (Phelan and Featherstone, 1997). PBX can modulate the affinity and stability of DNA binding and regulate transcriptional activity. The cooperative heterodimerization is carried out through a conserved protein motif found N-terminal to the Hox homeodomain (Slupsky et al., 2001; Huang et al., 2005). Interactions between PBX and HOX might also be mediated by residues of the N-terminal arm of HOX proteins (Shanmugam et al., 1997). It has been reported that PBX1 and HOXB1 can cooperatively activate the transcription through an autoregulatory element, directing spatially restricted expression of the HOXB1 gene (b1-ARE) in the developing hindbrain. However, only limited kinds of HOX can bind cooperatively with PBX (HOXA1, HOXB1, and HOXA2; Di Rocco et al.,

Contract grant sponsor: Japanese Ministry of Health, Labor and Welfare; Contract grant number: H14-kokoro-002; Contract grant sponsor: Japanese Ministry of Education, Culture Sports, Science and Technology; Contract grant number: 2005, 17659315; Contract grant number: 2004, 16012242.

*Correspondence to: Eiji Nanba, MD, PhD, Division of Functional Genomics, Research Center for Bioscience and Technology, Tottori University, 86 Nishi-machi, Yonago 683-8503, Japan.
E-mail: enanba@grape.med.tottori-u.ac.jp

Received 18 April 2006; Revised 4 October 2006; Accepted 5 October 2006

Published online 27 November 2006 in Wiley InterScience (www.interscience.wiley.com). DOI: 10.1002/jnr.21137

2001). This autoregulatory enhancer is the key regulatory element for the normal rhombomere 4 expression of Hoxb1 in the developing hindbrain, whereas Hoxa1 and Hoxb1 synergize in patterning the hindbrain cranial nerves and second pharyngeal arch (Gavalas et al., 1998).

HOXA1 is one of the first HOX genes to be expressed during embryonic development (Pearson et al., 2005). In mice, its expression starts from 7.5 dpc, and it is established in the neuroectoderm and mesoderm at 8.0 dpc. (Remacle et al., 2004). HOXA1 gene encodes two alternatively spliced mRNAs, which appear to be differentially expressed in the developing embryo. The homeodomain-containing variant 1 undergoes transcriptional activation during hindbrain development from E7 to E8.5 (Godwin et al., 1998). Functional inactivation of this gene results in prenatal lethality and numerous malformations (Lufkin et al., 1991; Carpenter et al., 1993). Hoxa1 null mice exhibit hindbrain segmentation and patterning defects that cause abnormal development of cranial nerve, cranial ganglia, and branchial arch derivatives (Chisaka et al., 1992). Furthermore, ectopic expression of Hoxa1 in transgenic mice leads to abnormalities of the developing hindbrain and ultimately results in embryonic death (Zhang et al., 1994).

HOXA1 gene contains a tract of 10-histidine repeat. In our previous study, we identified novel variants of polyhistidine tracts in HOXA1 gene in a Japanese population, and no homozygous case has been found for any of these variants (Paraguison et al., 2005). Certain individuals were heterozygous for deleted 7- and 9-histidine repeats and expanded 11- and 12-histidine repeats. Expression of expanded polyhistidine variants of HOXA1 proteins resulted in accelerated formation of ubiquitinated intranuclear aggregates and increased cell death. However, the mechanism by which this aggregation occurs is poorly understood. In this study, we showed that expression of expanded polyhistidine variants of HOXA1 in human neuroblastoma cell line SK-N-SH and embryonic carcinoma cell line P19 also caused increased intranuclear aggregation and cell death. However, there was a significant reduction of protein aggregation and cell death upon Rapamycin treatment, indicating involvement of the autophagic process. Expanded variants exhibited impaired cooperative binding with the cofactor PBX1, resulting in decreased transcriptional activity. Moreover, cells overexpressing expanded and deleted variants exhibited impaired neuronal differentiation. These data provide new insights on the function of polyhistidine variants of HOXA1 protein in neuronal cells.

MATERIALS AND METHODS

Antibodies and Reagents

The following antibodies were used: polyclonal goat anti-HOXA1 antibody (Santa Cruz Biotechnology, Santa Cruz, CA; sc-17146), monoclonal mouse anti-EGFP antibody (Santa Cruz Biotechnology, sc-9996), polyclonal rabbit anti-MAP2, H-300 (Santa Cruz Biotechnology, sc-20172), polyclonal rabbit anti PBX1, P-20 (Santa Cruz Biotechnology, sc-889), and polyclonal rabbit anti-β-tubulin H235 (Santa Cruz Biotechnology, sc-9104) and Alexa Fluor 594-conjugated anti-goat IgG, Alexa Fluor 555-conjugated anti-rabbit IgG, and Alexa Fluor 555-conjugated anti-mouse IgG (Molecular Probes, Eugene, OR). The following reagents were also used for this study: 10 μM retinoic acid (Sigma, St. Louis, MO; R2625) immediately after transfection, 10 mM 3-methyladenine (3-MA; Sigma, M9281) 15 hr prior to fixation, and 100 μM z-VAD-fink (Promega, Madison, WI; G7231) and 2 μg/ml Rapamycin (Sigma, R0395) both right after transfection.

Expression Vectors and Reporter Construct

Human HOXA1 expression vectors were generated as described previously (Paraguison et al., 2005). The following primer sets with suitable restriction enzyme recognition sites (Sac I and Bam HI) were used to generate HOXA1 variant 1: 5′- TAGAGCTCACCATGGACAATGCAAGAATGAACTCC-3′ and 5′-ATGGATCCGTGTGGGAGGTAGTCAGAGTGTCTGA-3′. All DNA amplification steps were performed using high fidelity Pfu Ultra DNA polymerase (Stratagene, La Jolla, CA) using genomic DNA and cDNA derived from human normal lymphoblast and confirmed by sequencing (ABI 3130xl). Expression constructs were derived from CMV promoter-based expression vector, pCMV-Script (Stratagene) and pEGFP-N1 (Invitrogen, San Diego, CA). The expression plasmids pCMV-Script and pEGFP-N1 were used as empty vector controls. The luciferase reporter construct pAdMLARE containing b1-ARE and the Pbx1 expression construct pSGPbx1a were generous gifts of Prof. Zappavigna (Di Rocco et al., 2001).

Cell Culture and Transfection

COS-7 cells, murine P19 embryonal carcinoma (EC) cells, and the human neuroblastoma cell line SK-N-SH were maintained in Dulbecco's modified Eagle's medium (DMEM; Sigma; D6429) supplemented with 10% fetal bovine serum (FBS; HyClone, Logan, UT). Cultures 50–80% confluent were transfected with Fugene 6 transfection reagent (Roche, Indianapolis, IN) in accordance with the manufacturer's recommendations. For a typical experiment, 1 μg of expression vector was used in a 35-mm culture dish. For cotransfection experiments, 1 μg of reporter plasmid (pAdMLARE), 0.5 μg of HOXA1 expression construct, 1 μg of PBX1 expression construct, and 0.3 μg of pEGFP as an internal control were used in a 35-mm dish. For Western blot analyses, cells cultured in 10-cm dishes were transfected with 10 μg of plasmid construct using Fugene-6 (Roche). To initiate differentiation, SK-N-SH cells were inoculated and treated with 10 μM retinoic acid (RA), whereas P19 cells were grown in a serum-free condition. Dead cells were scored under a fluorescence microscope (Leica DMIRE2).

Luciferase Assay

After 24 hr posttransfection, the cells were harvested and lysed in Pica Gene cell culture lysis reagent (Toyo Ink, Tokyo, Japan). Luciferase assay was carried out by using a Pica Gene kit (Toyo Ink) in accordance with the manufacturer's protocol. HOXA1 cooperative expression with PBX1

using pAdMLARE reporter construct was assessed by quantitative luciferase assay with Luminescencer-PSN (Bio-Instrument ATTO AB-220). pEGFP-N1 plasmid was used as an internal control.

Immunostaining, Dead Cell Scoring, and Imaging

The cells transiently expressing HOXA1 constructs were grown in 35-mm dishes containing glass coverslips. Cells attached to the glass coverslips were washed with phosphate-buffered saline (PBS), fixed with 4% paraformaldehyde, and incubated with antibodies as described previously (Paraguison et al., 2005). Confocal scanning analysis was performed with a Leica confocal microscope (Leica TCS-SP2). The degree of protein accumulation within the cell nuclei and the cytosol of transfected cells was scored. The cells were counted from 10 randomly selected microscope fields of each sample, 15 in the case of SK-N-SH cells. The ratio of the number of cells with protein aggregation over the total number of cells was then computed. Each experiment was performed independently in triplicate.

Western Blotting and Immunoprecipitation

Posttransfected cells were harvested and lysed by sonication in a buffer containing 10 mM Tris-HCl (pH 7.4), 150 mM NaCl, 1 mM EDTA, 1 mM EGTA, and protease inhibitor cocktail (Roche). Proteins were quantified by using a protein assay rapid kit (Wako, Osaka, Japan), run on 10% or 12% SDS-PAGE gels, and transferred on PVDF membranes (Millipore, Bedford, MA; IPVH00010) by a semidry blotter (Bio-Rad, Hercules, CA). Membranes were incubated with antibodies as described previously. Protein lysates from cotransfection experiments were immunoprecipitated with anti-GFP and used for Western blotting with anti-PBX1. Polyclonal rabbit anti-MAP2 antibody was used for quantifying neuronal differentiation in SK-N-SH. Signals were detected using ECL reagent (Amersham-Pharmacia Biotech, Arlington Heights, IL) on X-ray films (Fuji). For quantification, images were analyzed in NIH Image software.

RESULTS

Expanded Polyhistidine Variants of HOXA1 Enhanced Intranuclear Protein Aggregation in Neuronal Cell Lines

We have previously reported that expanded polyhistidine variants in HOXA1 resulted in early nuclear protein aggregation and an increased cell death in COS7 cells (Paraguison et al., 2005). Increasing polyhistidine repeat length coincided with early protein aggregation and accelerated cell death. In contrast, no significant difference was observed between cells overexpressing 7-polyhistidine variant and wild-type 10-polyhistidine repeat variant.

In the current study, we observed that these nuclear aggregations were also detected in both SK-N-SH cells (Fig. 1A) and P19 cells (Fig. 1B). To rule out the possibility that these aggregates were caused by enhanced green fluorescent protein (EGFP) tagging, transfection with untagged cytomegalovirus (CMV)-driven expression of HOXA1 variants was performed in COS-7 cells. Immunostaining with anti-HOXA1/Alexa 594 anti-goat also exhibited protein aggregates 18 hr posttransfection (Fig. 1C). After 18–20 hr, cells transfected with EGFP-tagged HOXA1 proteins were analyzed for Western blotting. In lysates of cells transfected with 11- and 12-polyhistidine variants, insoluble high-molecular-weight proteins remained in the stacking gel (Fig. 1D), indicative of protein complex accumulation.

Rapamycin Cleared Protein Aggregations and Decreased Cell Death in COS-7 Cells Expressing Expanded Variants of HOXA1, Whereas 3-MA Reversed This Effect

We also attempted to determine the type of cell death occurring as a consequence of expression of HOXA1 expanded polyhistidine variants. Recently, it has been reported that autophagic cell death was partially mediated by caspase activation (Ravikumar et al., 2006). Thus, we examined whether caspase inhibition could suppress cell death by using a cell-permeable pan caspase inhibitor, z-VAD-fmk, that binds to the catalytic site of caspase proteases and can inhibit induction of apoptosis (Broustas et al., 2004). However, no significant inhibition was seen in cells treated with 100 μM z-VAD-fmk (Fig. 2A,B). Thus, we speculated that classical apoptosis is not the mechanism involved in HOXA1-related cell death.

To understand better the mechanism responsible for clearance of protein aggregates, we examined the possible role of autophagy in degrading these proteins and the effect of caspase inhibition on cell death in COS-7 cells. During our time course experiments, we observed that aggregations were present not only in the nucleus but also in the cytosol at the early stages of expression (18 hr after transfection). These cytosolic aggregates were abundant in cells expressing the expanded 12-histidine variants of HOXA1-EGFP (Fig. 2C). Aggregates gradually cleared out by the endogenous autophagic mechanism of the cell and were concentrated in the nuclei at 42 hr after transfection (Fig. 2C,D). We explored the possible involvement of the autophagic process in the clearing of protein aggregates in these cells. 3-Methyladenine (3-MA), which has an inhibitory effect on autophagy (Ravikumar et al., 2002), enhanced nuclear aggregations and cell death (Fig. 2E,F). There is a decreased rate of clearance of protein aggregates observed in 3-MA-treated cells overexpressing 12-His variant. Cytosolic aggregates around the outer perinuclear periphery are noticeable in the later stage of expression, i.e., about 42 hr, where they were supposed to be cleared out in the 3-MA nontreated transfected cells (Fig. 2F). Conversely, rapamycin, an autophagy-inducing chemical (Ravikumar et al., 2006), decreased cytosolic and nuclear aggregation that eventually reduced cell death particularly in the expanded 12-histidine variant (Fig. 2G). This suggested that clearing of HOXA1-EGFP protein aggregates was mediated by an autophagic mechanism. We

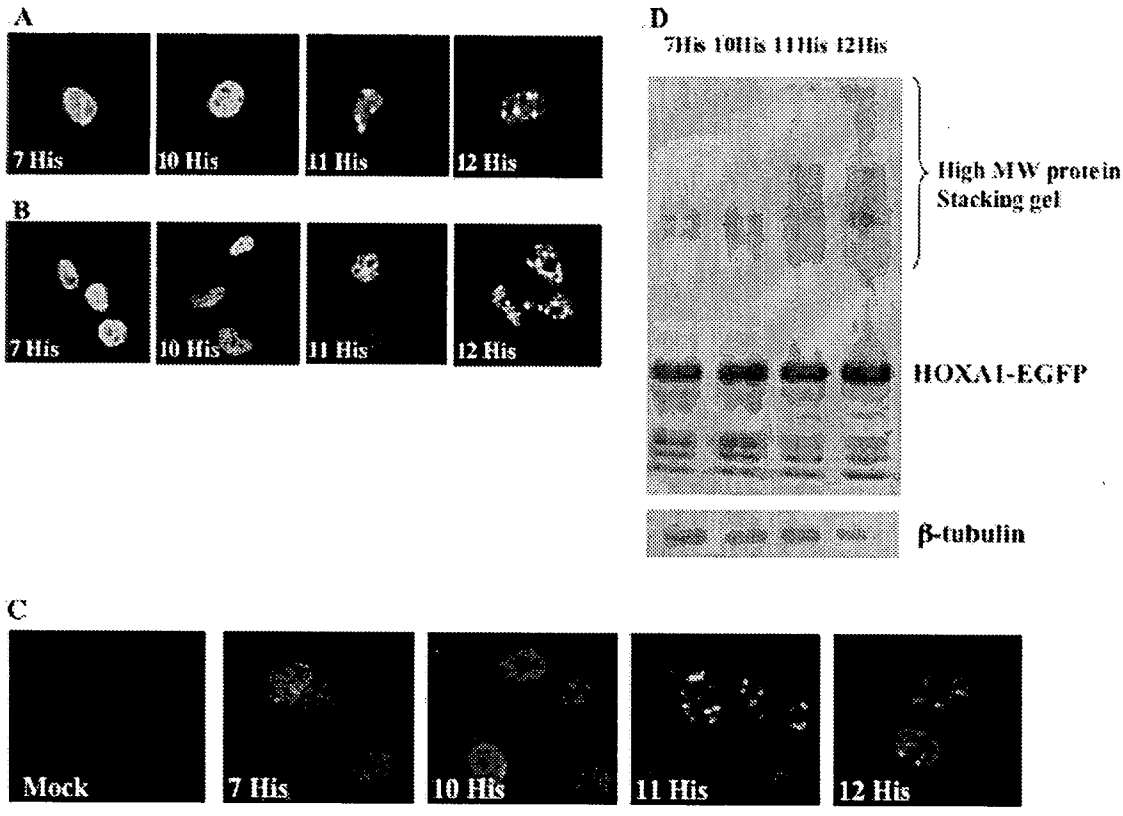

Fig. 1. Expression of HOXA1 polyhistidine expansion variants results in protein aggregation. HOXA1-EGFP construct variants were expressed in neuronal cell lines. As early as 15–20 hr after transfection, intranuclear aggregates were already detected in cells transfected with expanded HOXA1 variant. Images were taken 18 hr after transfection. EGFP fluorescent signals were visualized by confocal microscopy. **A:** Neuroblastoma cells, SK-N-SH. **B:** Embryonic carcinoma cells, P19. **C:** COS-7 cells transfected with untagged HOXA1 and immunostained with anti-HOXA1/Alexa 594 anti-goat (red signals). Fluorescence images were taken 18 hr posttransfection. **D:** 18–24-hr posttransfected cell lysates analyzed for Western blotting using anti-GFP. An increased amount of high-molecular-weight SDS-insoluble protein was detected in the stacking gel in lanes of expanded HOXA1, indicating that the length of histidine repeats is directly proportional with the degree protein accumulations. [Color figure can be viewed in the online issue, which is available at www.interscience.wiley.com.]

further noted that the autophagic clearing system was more efficient in degrading cytosolic aggregates, since autophagic vacuoles were directly accessible in the cytosol. However, the increased production of accumulated intranuclear proteins might have overloaded the autophagic clearing mechanism, thus resulting in cell death.

Fig. 2. Protein aggregations in the cytosol are cleared by an autophagic process. **A:** Right after transfection, cells were treated with 100 μM z-VAD-fmk and scored after 24 hr postransfection. z-VAD-fmk did not inhibit intranuclear protein aggregation. Mock EGFP served as a negative control. **B:** Fluorescence images of EGFP and HOXA1-EGFP 12-His variant treated with z-VAD-fmk. **C:** COS-7 cells were transfected with HOXA1-EGFP constructs at 18 hr post-transfection; cytosolic aggregates could be seen abundantly in cells transfected with HOXA1-EGFP 12-histidine variant. These aggregates were eventually cleared out after 42 hr and were mostly concentrated in the nuclei. **D:** Graph showing percentage of cells with protein aggregation and dead cells per number of EGFP-positive transfected cells at 18 and 42 hr after transfection. **E:** Transfected cells were treated with 10 mM 3-methyladenine (3-MA) 15 hr prior to fixation. HOXA1-EGFP 10-His variant-transfected cells were treated with DMSO to serve as a control for cell toxicity. 3-MA increases protein aggregations and cell death in HOXA1-EGFP-transfected COS-7 cells. Dead cells and those exhibiting nuclear and cytosolic aggregation were scored 18 hr after transfection. **F:** No protein aggregation was detected in mock-EGFP-transfected COS-7 cells treated with 3-MA; however, an increase in cell death was observed. HOXA1-EGFP 12-His variant exhibited cytosolic aggregates around the outer perinuclear periphery, which are denoted by arrows. **G:** Immediately after transfection, 10-His and 12-His repeat variants of HOXA1-EGFP-transfected COS-7 cells were treated with 2 μg/ml Rapamycin prior to fixation. Rapamycin reduces cytosolic aggregation and cell death significantly in the cells transfected with 12-His repeat variant. Dead cells and protein aggregations were scored 42 hr after transfection. Error bars represent SEM; n = 3. $*P < 0.05$, $**P < 0.01$. P values from a paired t-test in all experiments. [Color figure can be viewed in the online issue, which is available at www.interscience.wiley.com.]

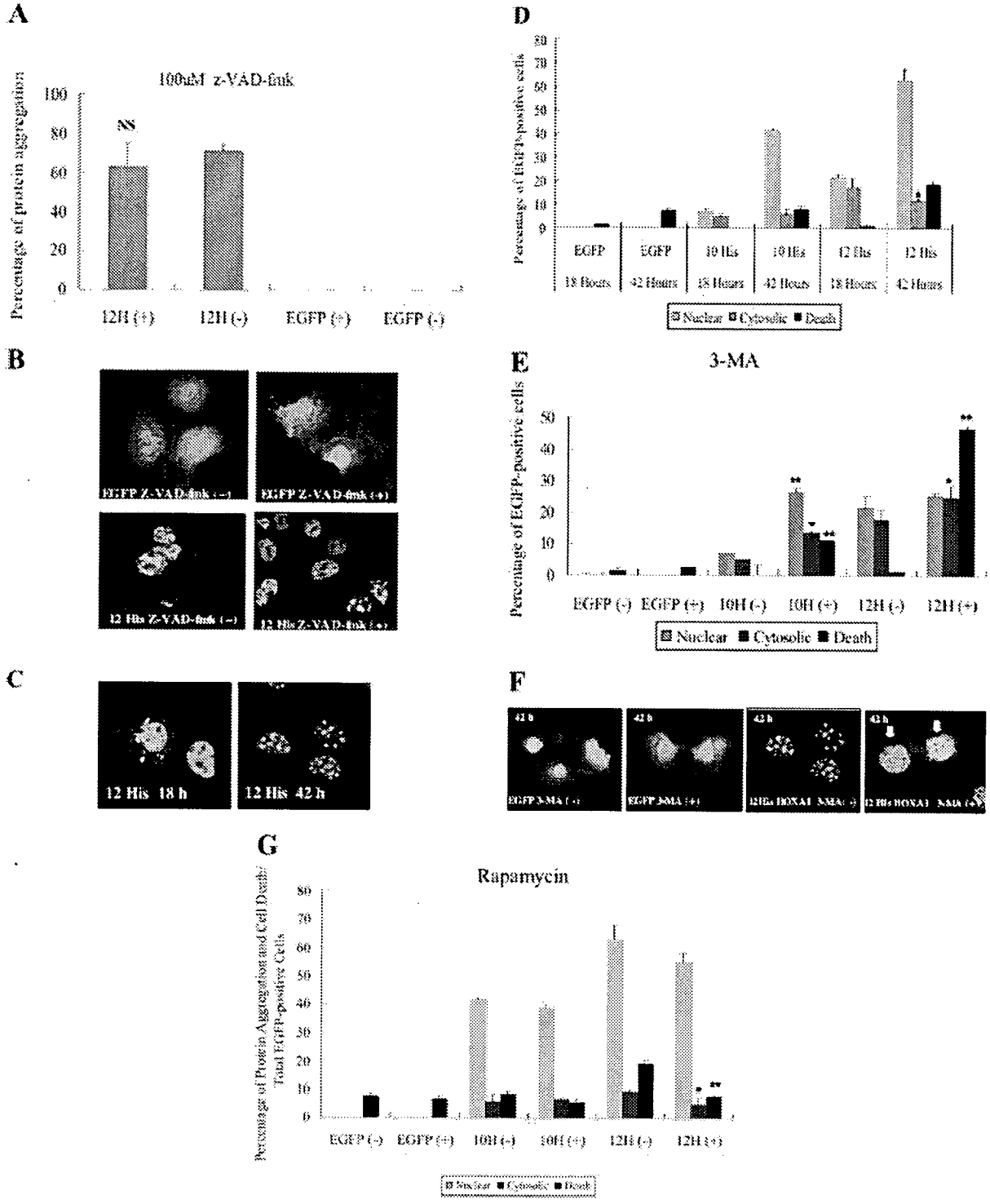
A
100nM z-VAD-fmk
Percentage of protein aggregation
NS
12H (+)
12H (-)
EGFP (+)
EGFP (-)
B
EGFP Z-VAD-fmk (-)
EGFP Z-VAD-fmk (+)
12 His Z-VAD-fmk (-)
12 His Z-VAD-fmk (+)
C
12 His 18 h
12 His 42 h
D
Percentage of EGFP-positive cells
EGFP 18 Hours
EGFP 42 Hours
10 His 18 Hours
10 His 42 Hours
12 His 18 Hours
12 His 42 Hours
Nuclear
Cytosolic
Death
E
3-MA
Percentage of EGFP-positive cells
EGFP (-)
EGFP (+)
10H (-)
10H (+)
12H (-)
12H (+)
Nuclear
Cytosolic
Death
F
G
Rapamycin
Percentage of Protein Aggregation and Cell Death/ Total EGFP-positive Cells
EGFP (-)
EGFP (+)
10H (-)
10H (+)
12H (-)
12H (+)

Figure 2.

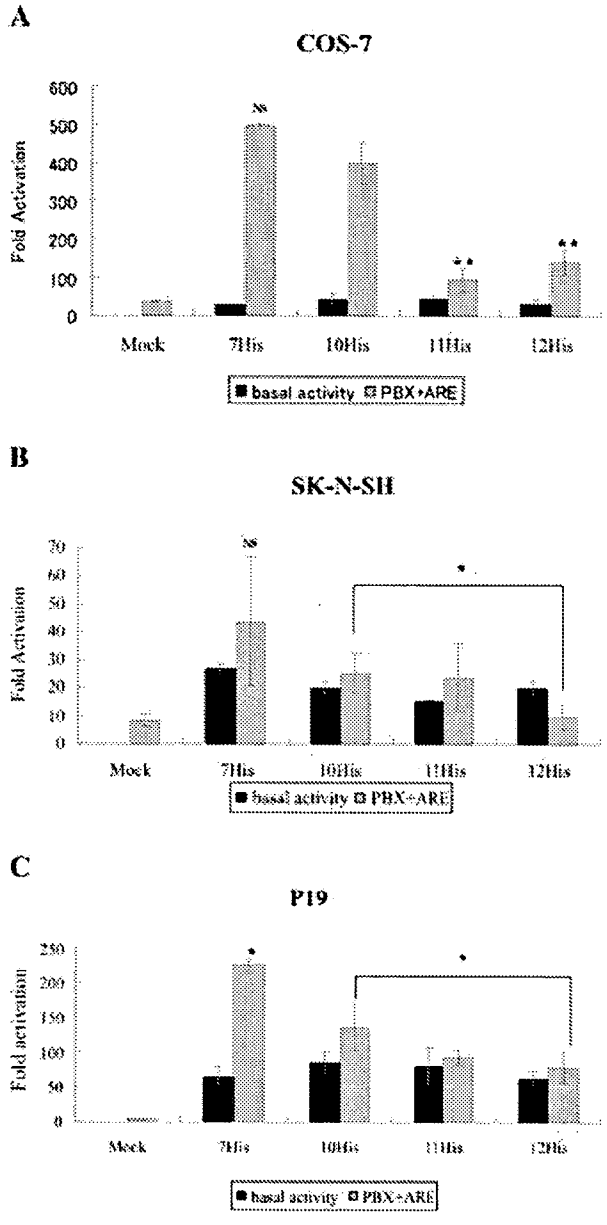

Fig. 3. Expanded HOXA1 reduces PBX1-coupled transcriptional activity. Luciferase assay from the different cell lines. Cells were cotransfected with plasmids containing PBX1, HOXA1, and the enhancer b1-ARE fused to a luciferase reporter gene (Di Rocco et al., 2001). EGFP vector was used as an internal control. **A:** COS-7. **B:** Neuroblastoma cell line SK-N-SH. **C:** Embryonic carcinoma cell line P19 grown in serum-free medium. Bars represent the mean ± SE of at least three independent experiments. $*P < 0.05$, $**P < 0.01$.

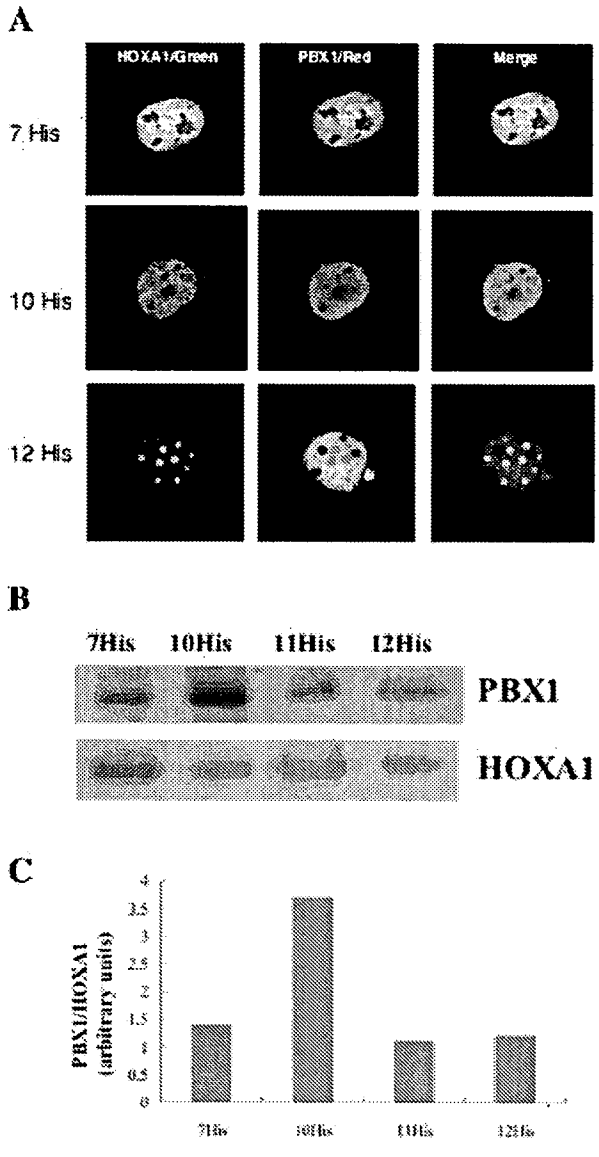

Fig. 4. HOXA1 and PBX1 interaction is impaired in expanded variant of HOXA1. **A:** Immunofluorescence images of COS-7 cotransfected with PBX1, an enhancer bi-ARE, and 7-His, 10-His, or 12-His repeat variants of HOXA1-EGFP. Fluorescence images were taken 24 hr posttransfection. Red signals: anti-PBX1. Note the absence of PBX1 signal in protein aggregates of the 12-His variant. **B:** Immunoprecipitation with anti-GFP and Western blotted with anti-PBX1 and anti-HOXA1. PBX1 protein shows decreased levels in both expanded and deleted variants of HOXA1-EGFP transfected to COS-7 cells. **C:** Quantification of bound PBX1 protein levels per HOXA1 protein from Western blot analysis. [Color figure can be viewed in the online issue, which is available at www.interscience.wiley.com.]

Transcriptional Activities of Polyhistidine Variants of HOXA1 Coupled With PBX1

We next examined the physiological relevance of polyhistidine variants of HOXA1 protein in neuronal cells. PBX1 plays a major role in cooperative transcriptional activation with HOXA1 through an autoregulatory element, the b1-ARE (Di Rocco et al., 2001). To investigate the cooperative transcription of PBX1 with

the different variants of HOXA1 through b1-ARE, we simultaneously expressed HOXA1, PBX1, EGFP (an internal control), and b1-ARE luciferase reporter constructs in COS7, SK-N-SH, and P19 cells. Luciferase assay were performed 24 hr after transfection. The P19 embryonic cell line was grown under serum-free conditions. Growth in serum-free media itself committed EC cells to neural differentiation (Darmon et al., 1981) and addition of retinoic acid (RA) intensified this effect (Tanaka et al., 1992). However, nonneural cell types arise after treatment with RA under serum-containing conditions. Differentiation in serum-free media alone is accompanied by expression of only neuroectodermal/neural mRNAs, but treatment with RA invariably induces the cells to express both neuroectodermal/neural and endodermal mRNAs (Pachernik et al., 2005), so the serum-free medium condition was used in this experiment.

The transcriptional activities of expanded variants were significantly reduced in all cell lines, whereas the activities of deleted variant with 7-polyhistidine were enhanced in P19 cells compared with the activity of 10-polyhistidine variant (Fig. 3A–C). Immunofluorescence images revealed the inability of aggregated forms of expanded HOXA1 protein to bind efficiently with PBX1 protein (Fig. 4A). Inefficient interaction between expanded HOXA1 and PBX1 is clearly indicated by low levels of PBX1 protein in immunoprecipitation assay with anti-GFP (Fig. 4B,C).

Expanded and Deleted Polyhistidine Variants in HOXA1 Inhibited Neuronal Differentiation

Because HOXA1 is one of the neurodevelopmental genes, we examined whether polyhistidine variants had any effect on the process of neuronal differentiation. To accomplish this, RA-induced neuronal differentiation was performed in SK-N-SH cells. Phase microscopy shows the effect of RA treatment on the neurites of these cells (Fig. 5A). Immunocytochemistry with antibody against the neuron-specific protein MAP2 revealed neurite outgrowth in cells expressing the 10-histidine HOXA1-GFP, 42 hr after transfection (Fig. 5B). In contrast, a greater number of cells expressing expanded and deleted forms of HOXA1-GFP failed to initiate neurite outgrowth. Total levels of MAP2 protein in cells overexpressing expanded and deleted variants were also significantly reduced (Fig. 5C,D). The appearance of

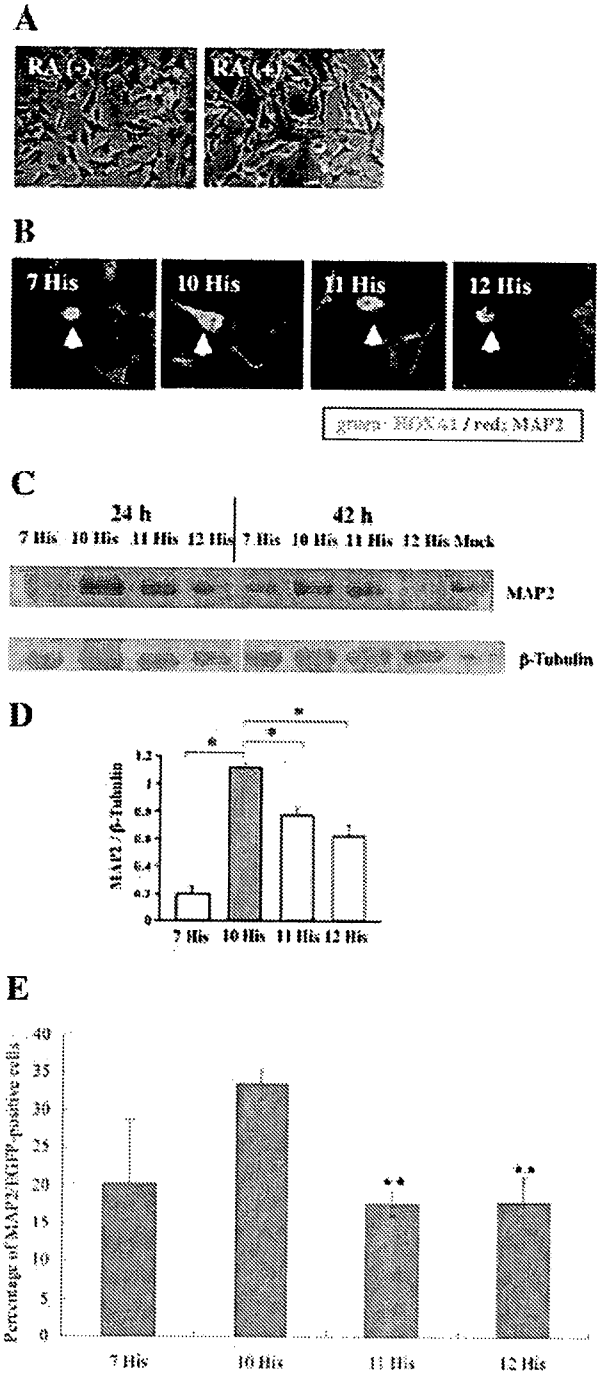

Fig. 5. Expanded and deleted polyhistidine repeats in HOXA1 inhibit neuronal differentiation. **A:** Retinoic acid (RA)-induced neuronal differentiation in SK-N-SH cells Phase images of SK-N-SH cells treated with (right) or without (left) 10 μM RA for 42 hr. **B:** HOXA1-EGFP-transfected SK-N-SH treated with 10 μM RA for 42 hr. Immunofluorescence images where taken 42 hr after transfection. Expanded 11- and 12-His repeat variants as well as deleted 7-His repeat variants inhibit neuronal differentiation. Note the neurite outgrowth immunostained with MAP2 (red signal). **C:** Western blot analysis shows decreased MAP2 expression levels in the expanded and deleted forms. **D:** Quantification of MAP2 expression levels normalized with β-tubulin. **E:** Quantification of the percentage of EGFP-MAP2-double-positive cells. Error bars represent SEM; n = 3. $*P < 0.05$, $**P < 0.01$. *P* values from a paired *t*-test in all experiments. [Color figure can be viewed in the online issue, which is available at www.interscience.wiley.com.]

differentiated cells was also examined by scoring MAP2-positive transformants expressing the HOXA1-EGFP variants. EGFP-MAP2 double-positive cells quantification also confirmed that there is a significant decrease in the percentage of MAP2 levels particularly in the expanded variants.

DISCUSSION

In this current study, we have shown that polyhistidine repeat tract variants compromised HOXA1 function in transcription and neuronal differentiation. Moreover, we have presented evidence that cell death resulting from polyhistidine repeat expansion is mediated primarily by authophagy and not by a caspase-dependent mechanism. Authophagy is a type of cell death involving bulk degradation of cytoplasmic proteins or organelles in the lytic compartment. Inhibition of autophagy enhances protein aggregation and cell death (Ravikumar et al., 2002). Our data showed that 3-MA accelerates protein accumulations and enhances cell death, particularly in the expanded variants (Fig. 2E,F). Conversely, Rapamycin, an inducer of the autophagic process, decreases protein aggregates and reduces cell death (Fig. 2G). Taken together, our findings indicate that autophagy is involved in the degradation and clearance of aggregations of expanded HOXA1 variants.

HOXA1 splice variant 1 is reported to be active in E7–E8.5 and functions in the presumptive rhombomere 3 and 4 regions of the developing hindbrain (Zhang et al., 1994). However, the nonhomeodomain-containing variant is expressed in the endodermal derivative after E8.5 to the adult stage (Godwin et al., 1998). Therefore, we speculate that splice variant 1 may be active only in early stages of embryonic neurodevelopment. As one of the DNA-binding proteins and transcription factors in the HOX gene family, HOXA1 also relies on the activity of transcriptional cofactors aside from its DNA-binding properties (Pearson et al., 2005). A previous study has reported that HOXB1 and PBX1 cooperatively activate transcription under the control of b1-ARE (autoregulatory enhancer). Moreover, HOXA1 and HOXA2 are also able to activate transcription by b1-ARE in cooperation with PBX1 (Di Rocco et al., 2001). We examined the binding ability of our HOXA1 variants to PBX1 and b1-ARE by evaluating the cooperative transcriptional activation using a luciferase assay. Expanded variants transfected into COS-7 as well as SK-N-SH neuroblastoma and P19 embryonic carcinoma cells (EC) that were induced to undergo neuronal differentiation indeed showed significantly reduced activation compared with the wild type, whereas the deleted variant expressed in P19 cell line showed an enhanced activation (Fig. 3). However, the reason for increased transcriptional activity observed in the deleted variant in this cell line is as yet unknown. Immunofluorescence images and immunoprecipitation assay clearly confirmed the inability of aggregated forms of expanded HOXA1 protein to bind efficiently with PBX1 protein. The cooperative interaction between Hox and Pbx is mediated by a conserved hexapeptide sequence located toward the N-terminal region from Hox homeodomain (Phelan and Fetherstone, 1997; Remacle et al., 2004). Our results suggest that polyhistidine variants in HOXA1 might also affect the binding efficiency of its homeodomain to certain cofactors and/or other target genes or proteins.

Human neuroblastoma SK-N-SH cells, from a malignant pediatric tumor derived from the neural crest, retains its ability to differentiate into the neuronal lineage when exposed to RA (Wainwright et al., 2001). HOXA1 is the first target gene activated by RA, followed by a sequential activation of other HOX genes (Simeone et al., 1990; Martinez-Ceballos et al., 2005). We showed an inhibition of neuronal differentiation by not only the extended but also the deleted variants (Fig. 5). Our study provides novel insights on the pathological implications of the polyhistidine tract in HOXA1 and leaves us with the intriguing possibility that polyhistidine repeat expansions and deletions may cause aberrations in neuronal morphogenesis or differentiation in general.

EC cells differentiate into various lineages depending on the presence of activators in the culture medium (Pachernik et al., 2005). Growth under serum-free conditions committed EC cells to neural differentiation. Differentiation of EC cells into endodermal-like cells is induced by serum. Interestingly, we found that, in EC cells committed to neural differentiation, transcriptional activity inversely coincided with polyhistidine repeat length. These results further strengthen our theory that polyhistidine length affects neurodevelopment. In agreement with our results, another study has proposed that HOXA1 may function as a stimulator of neuroectodermal and mesodermal differentiation and a repressor of embryonic endoderm formation (Martinez-Ceballos et al., 2005) and that aberration in HOXA1 could lead to increased expression of endodermal genes by RA and would lead to repression of neuroectodermal and mesodermal markers. Premature death of HOXA1-expressing cells may impair transcription and neuronal differentiation.

Recently, Tischfield and colleagues (2005) reported that patients with Bosley-Salih-Alohrainy syndrome were homozygous for HOXA1 truncating mutations, whereas heterozygotes had normal phenotypes. This mutation resulted in abnormal development of the central nervous system in the brainstem. Distinguishing phenotypes include horizontal gaze abnormalities, mental retardation, and autism spectrum disorder. Even low levels of Hoxa1 expression in Hoxa1$^{+/-}$ cells are sufficient for normal activation of the Hoxa1 pathway and may explain why mice heterozygous for HOXA1 mutations appear normal (Pasqualetti et al., 2001; Martinez-Ceballos et al., 2005). In our previous report, we identified heterozygous polyhistidine repeat variants in HOXA1 gene from a Japanese population comprising normal and autistic individuals. No individuals homozygous for these mutations have been found. We speculate that there is a possibility

that phenotypic aberrations may exist in homozygous individuals. Future in vivo studies are essential to examine the physiological functions of the polyhistidine variants of HOXA1.

ACKNOWLEDGMENTS

We thank Prof. Vincenzo Zappavigna for providing the PBX1 and pAdMLARE reporter plasmids. R.C.P. is the recipient of a research scholarship from the Japanese Ministry of Education, Culture, Sports, Science and Technology.

REFERENCES

Broustas CG, Gokhale PC, Rahman A, Dritschlo A, Ahmad I, Kasid U. 2004. BRCC2, a novel BH3-like domain-containing protein, induces apoptosis in a caspase-dependent manner. J Biol Chem 279:26780–26788.

Carpenter EM, Goddard JM, Chisaka O, Manley NR, Capecchi MR. 1993. Loss of Hoxa1 (Hox-1.6) function results in the reorganization of the murine hindbrain. Development 118:1063–1075.

Chisaka O, Musci TS, Cappecchi MR. 1992. Developmental defects of the ear, cranial nerves and hindbrain resulting from targeted disruption of the mouse homeobox gene, Hox-1.6. Nature 355:516–520.

Darmon M, Bottenstein J, Sato G. 1981. Neural differentiation following culture of embryonal carcinoma cells in a serum-free defined medium. Dev Biol 85:463–473.

Di Rocco G, Gavalas A, Popperl H, Krumlauf R, Mavilio F, Zappavigna V. 2001. The recruitment of SOX/OCT complexes and the differential activity of HOXA1 and HOXB1 modulate the Hoxb1 auto-regulatory enhancer function. J Biol Chem 276:20506–20515.

Gavalas A, Studer M, Lumsden A, Rijli FM, Krumlauf R, Chambon P. 1998. Hoxa1 and Hoxb1 synergize in patterning the hindbrain, cranial nerves and second pharyngeal arch. Development 125:1123–1136.

Gehring WJ, Affolter M, Burglin T. 1994. Homeodomain proteins. Annu Rev Biochem 63:487–526.

Godwin AR, Stadler HS, Nakamura K, Cappecchi MR. 1998. Detection of targeted GFP-Hox gene fusions during mouse embryogenesis. Proc Natl Acad Sci U S A 95:13042–13047.

Grier DG, Thompson A, Kwasniewska A, McGonigle GJ, Halliday HL, Lappin TR. 2005. The pathophysiology of HOX genes and their role in cancer. J Pathol 205:154–171.

Huang H, Rastegar M, Bodner C, Goh SL, Rambaldi I, Featherstone M. 2005. MEIS C termini harbor transcriptional activation domains that respond to cell signaling. J Biol Chem 280:10119–10127.

Lufkin T, Dierich A, LeMeur M, Chambon M. 1991. Disruption of the Hox-1.6 homeobox gene results in defects in a region corresponding to its rostral domain of expression. Cell 66:1105–1119.

Martinez-Ceballos E, Chambon P, Gudas LJ. 2005. Differences in gene expression between wild type and Hoxa1 knockout embryonic stem cells after retinoic acid treatment or LIF removal. J Biol Chem 280: 16484–16498.

Pachernik J, Bryja V, Esner M, Kubala L, Dvorak P, Hampl A. 2005. Neural differentiation of pluripotent mouse embryonic carninoma cells by retinoic acid: inhibitory effects of serum. Physiol J 54:115–122.

Paraguison RC, Higaki K, Sakamoto Y, Hashimoto O, Miyake N, Matsumoto H, Yamamoto K, Sasaki T, Kato N, Nanba E. 2005. Polyhistidine tract expansions in HOXA1 result in intranuclear aggregation and increased cell death. Biochem Biophys Res Commun 336:1033–1039.

Pasqualetti M, Neun R, Davenne M, Rijli FM. 2001. Retinoic acid rescues inner ear defects in Hoxa1 deficient mice. Nat Genet 1:34–39.

Pearson JC, Lemons D, McGinnis W. 2005. Modulating hox gene functions during animal body patterning. Nat Rev Neurosci 6:893–904.

Phelan ML, Featherstone MS. 1997. Distinct HOX N-terminal arm residues are responsible for specificity of DNA recognition by HOX monomers and HOX-PBX heteromers. J Biol Chem 272:8635–8643.

Ravikumar B, Duden R, Rubinsztein DC. 2002. Aggregate-prone proteins with polyglutamine and polyalanine expansions are degraded by autophagy. Hum Mol Genet 11:1107–1117.

Ravikumar B, Berger Z, Vacher C, O'Kane CJ, Rubinszten DC. 2006. Rapamycin pre-treatment protects against apoptosis. Hum Mol Genet 15:1209–1216.

Remacle S, Abbas L, De Backer O, Pacico N, Gavalas A, Gofflot F, Picard JJRezsohazy R. 2004. Loss of function but no gain of function caused by amino acid substitutions in the hexapeptide of Hoxa1 in vivo. Mol Cell Biol 24:8567–8575.

Shanmugam K, Featherstone MS, Saragovi HU. 1997. Residues flanking the HOX YPWM motif contribute to cooperative interactions with PBX. J Biol Chem 272:19081–19087.

Simeone A, Acampora D, Arcioni L, Andrews PW, Boncinelli E, Mavilio F. 1990. Sequential activation of HOX 2 homeobox genes by retinoic acid in human embryonal carcinoma cells. Nature 346:763–766.

Slupsky CM, Sykes DB, Gay GL, Sykes BD. 2001. The HoxB1 hexapeptide is a prefolded domain: implications for the Pbx1/Hox interaction. Prot Sci 10:1244–1253.

Tanaka Y, Kawahata K, Nakata T, Hirokawa A. 1992. Chronological expression of microtubule-associated proteins (MAPs) in EC cell P19 after neural induction by retinoic acid. Brain Res 596:269–278.

Tischfield MA, Bosley TM, Salih MAM, Alorainy IA, Sener EC, Nester MJ, Oystreck DT, Chan WM, Andrews C, Erickson RP, Engle EC. 2005. Homozygous HOXA1 mutations disrupt human brainstem, inner ear, cardiovascular and cognitive development. Nat Genet 37: 1035–1037.

Wainwright LJ, Lasorella A, Iavarone A. 2001. Distinct mechanisms of cell cycle arrest control the decision between differentiation and senescence in human neuroblastoma cells. Proc Natl Acad Sci U S A 98: 9396–9400.

Zhang M, Kim HJ, Marshall H, Gendron-Maguire M, Lucas DA, Baron A, Gudas T, Gridley LJ, Krumlauf R, Grippo JF. 1994. Ectopic Hoxa-1 induces rhombomere transformation in mouse hindbrain. Development 120:2431–2442.

Available online at www.sciencedirect.com
ScienceDirect
Progress in Neuro-Psychopharmacology & Biological Psychiatry 31 (2007) 940–943
Progress In Neuro-Psychopharmacology & Biological Psychiatry
www.elsevier.com/locate/pnpbp

No association between the Neuronal Pentraxin II gene polymorphism and autism

Tetsuya Marui [a,*], Shinko Koishi [b], Ikuko Funatogawa [c], Kenji Yamamoto [d], Hideo Matsumoto [e], Ohiko Hashimoto [f], Michiko Ishijima [a], Eiji Nanba [g], Hisami Nishida [h], Toshiro Sugiyama [b], Kiyoto Kasai [a], Keiichiro Watanabe [a], Yukiko Kano [a], Nobumasa Kato [a], Tsukasa Sasaki [a,i]

[a] *Department of Neuropsychiatry, Graduate School of Medicine, University of Tokyo, 7-3-1 Hongo, Bunkyo, Tokyo 113, Japan*
[b] *Aichi Children's Health and Medical Center, Obu, Japan*
[c] *Department of Hygiene and Public Health, Teikyo University School of Medicine, Tokyo, Japan*
[d] *Department of Psychiatry, Kitasato University School of Medicine, Sagamihara, Japan*
[e] *Department of Psychiatry, Tokai University School of Medicine, Isehara, Japan*
[f] *Department of Occupational Therapy, Faculty of Nursing and Rehabilitation, Aino University, Ibaraki, Japan*
[g] *Gene Research Center, Tottori University, Yonago, Japan*
[h] *Asunaro Hospital for Child and Adolescent Psychiatry, Tsu, Japan*
[i] *Department of Psychiatry, Health Service Center, University of Tokyo, Tokyo, Japan*

Received 10 July 2006; received in revised form 26 February 2007; accepted 27 February 2007
Available online 3 March 2007

Abstract

Autism (MIM 209850) is a neurodevelopmental disorder characterized by difficulties with verbal and non-verbal communication, impairments in reciprocal social interactions, and displays of stereotypic behaviors, interests and activities. Twin and family studies have indicated a robust role of genetic factors in the development of autism.

Neuronal Pentraxin II (NPTX2) is located in chromosome 7q21.3-q22.1, where it is a candidate region for autism. NPTX2 promotes neuritic outgrowth and is suggested to mediate uptake of degraded synaptic material during synapse formation and remodeling. NPTX2 is also associated with the clustering of synaptic AMPA receptors. It was reported that glutamate systems including AMPA receptor was associated to the pathophysiology of autism. Thus, the NPTX2 gene is involved in neuritic outgrowth, synapse remodeling and the aggregation of neurotransmitter receptors at synapses. These functions play an important role in the mechanisms of learning and brain development.

In the present study, we tested for the presence of the association of four single nucleotide polymorphisms (SNPs) of NPTX2 and haplotypes consisting of the SNPs with autism, between autistic patients (n=170) and normal controls (n=214) in a Japanese population. No significant difference was observed in the allele, genotype or haplotype frequencies between the patients and controls. Thus, the NPTX2 locus is not likely to play a major role in the development of autism. However, further studies with larger sample size and sequencing of NPTX2 gene are needed to exclude a role of NPTX2 gene in autism.

Keywords: Association study; Autistic disorder; Chromosome 7q; Haplotype block; NPTX2 gene; SNPs

1. Introduction

Autism (MIM 209850) is a neurodevelopmental disorder characterized by difficulties with verbal and non-verbal communication, impairments in reciprocal social interactions, and displays of stereotypic behaviors, interests and activities. Twin and family studies have indicated a robust role of genetic factors

Abbreviations: AMPA, alpha-amino-3-hydroxy-5-mathyl-4-isoxazole propionic acid; CBQ-R, the Child Behavior Questionnaire Revised; CRP, C-reactive protein; DSM-IV, the Diagnostic and Statistical Manual of Mental Disorders, Fourth Edition; NPTX2, Neuronal Pentraxin II; SNPs, single nucleotide polymorphisms.

* Corresponding author. Tel.: +81 3 5800 9263; fax: +81 42 379 4544.
E-mail address: PXX03135@nifty.ne.jp (T. Marui).

0278-5846/$ - see front matter © 2007 Elsevier Inc. All rights reserved.
doi:10.1016/j.pnpbp.2007.02.016

in the development of autism (Folstein and Rosen-Sheidley, 2001). The respective concordance rates of the disorder in monozygotic and dizygotic twins were reported to be 91 and 0% (Steffenburg et al., 1989) and 60 and 0% (Bailey et al., 1995). Statistical models suggest that between 2 and 10 (Pickles et al., 1995) or more than 15 (Risch et al., 1999) loci are probably implicated. Although the results of the linkage studies were controversial, several studies have provided evidence for a chromosomal 7q region as a susceptibility locus (or loci) of autism (Folstein and Rosen-Sheidley, 2001).

Neuronal Pentraxin II (NPTX2), located in chromosome 7q21.3-q22.1, is a member of the pentraxins that include the C-reactive protein (CRP) (Hsu and Perin, 1995). NPTX2 gene is 11 kb long and contains 4 introns (Hsu and Perin, 1995). It was found that NPTX2 promoted neuritic outgrowth (Tsui et al., 1996), and is suggested to mediate uptake of degraded synaptic material during synapse formation and remodeling (Dodds et al., 1997; Kirkpatrick et al., 2000). NPTX2 is expressed at relatively high levels in the developing and adult brain (Tsui et al., 1996). It was also reported that NPTX2 was expressed in a subset of axons and dendrites in cultured spinal and hippocampal neurons (O'Brien et al., 1999). NPTX2 may play a critical role in the organization of excitatory synapses. It was also shown that NPTX2 is selectively enriched at some excitatory synapses of spinal cord and hippocampal neurons in vitro (O'Brien et al., 1999).

Genetic, neuroimaging, postmortem and pharmacologic treatment approaches have suggested that neurochemical contributions of glutamate systems to the pathophysiology of autism. Alpha-amino-3-hydroxy-5-mathyl-4-isoxazole propionic acid (AMPA) included in the glutamate systems may be involved in the pathogenesis of the disorder (Carlsson, 1998). The predominant charge carrier during routine fast excitatory synaptic transmission is the alpha-amino-3-hydroxy-5-mathyl-4-isoxazole propionic acid (AMPA) type receptor (Hollmann and Heinemann, 1994). NPTX2 is associated with the clustering of synaptic AMPA receptors (O'Brien et al., 1999).

Thus, the NPTX2 gene is involved in neuritic outgrowth, synapse remodeling and the aggregation of neurotransmitter receptors at synapses. These functions play an important role in the mechanisms of learning and brain development. However, to our knowledge, no study has been reported between the NPTX2 gene and autism. In the present study, we tested for the presence of association of four single nucleotide polymorphisms (SNPs) of NPTX2 and haplotypes consisting of the SNPs with autism, using case-control design.

2. Subjects and methods

The patients comprised 170 unrelated Japanese with autism (147 males and 23 females, mean age=20.8 years within a range of 3–41 years). The patients were recruited from the outpatient clinics of the departments of psychiatry, Tokyo University Hospital and Tokai University Hospital, and seven daycare facilities for subjects with developmental disorders. All the hospitals and facilities were located around Tokyo. All the subjects met the DSM-IV criteria for autistic disorder. The diagnoses were made by one or two experienced child psychiatrists through interviews and reviews of clinical records. Apparent physical anomalies were not observed in the subjects. The controls consisted of 214 unrelated Japanese healthy volunteers (145 males and 69 females, mean age=34.6 years within a range of 21–65 years). They were mainly recruited from the hospital and facility staff, and all of them resided in the same area (Kanto District or around Tokyo) as the patients. All the patients and controls were ethnically Japanese, with no parents or grandparents of ethnicity other than Japanese.

Confirmation of the diagnosis was conducted as follows. Semi-structured behavior–observation of the patients and interviews of them and their parents were conducted for most of the cases by two experienced child psychiatrists independently. At the interview of the parent(s), the Child Behavior Questionnaire Revised (CBQ-R) (Izutsu et al., 2001) was used to assist evaluation of autism-specific behaviors and symptoms. After the initial observation and interview, we followed up by examining the patients' behavior and symptoms for several months (for at least six months in most of the cases) and those who were not considered to meet the Diagnostic and Statistical Manual of Mental Disorders, Fourth Edition (DSM-IV) criteria during the follow-up were excluded from the sample.

The present study was approved by the Ethical Committee, the Faculty of Medicine of the University of Tokyo and Tokai University. The objective of the present study was clearly expressed and written informed consent was obtained from all subjects and healthy volunteers.

Table 1
Allele frequencies of 4 SNPs of the NPTX2 gene in autism patients and controls

Locus	db SNP ID	Allele[a]	Minor allele frequencies				Chi-square	p-value	Odds ratio	95% confidence intervals		Chromosome position	Location
			Patients		Controls					Lower	Upper		
			N	%	N	%							
SNP-1	rs2291273	C/T	29	9%	37	11%	0.00	0.951	1.02	0.61	1.69	97893940	Intron02
SNP-2	rs1681248	G/C	66	20%	75	22%	0.38	0.536	1.12	0.78	1.62	97898498	Intron02
SNP-3	rs705318	G/T	136	40%	166	49%	0.06	0.801	0.96	0.72	1.29	97900986	Intron03
SNP-4	rs705315	G/A	67	20%	81	24%	0.09	0.766	1.06	0.74	1.52	97903387	3'UTR

Chromosome position of the SNPs is according to the NCBI Ref Seq.
[a] The alleles are listed as major/minor allele.

Peripheral blood was obtained and genomic DNA was extracted using the standard phenol-chloroform method. Single nucleotide polymorphisms (SNPs) were analyzed, using the ABI 7900HT sequence detective system (Applied Biosystems, Foster City, CA, USA). The primers and probes of the ABI Assays-on-Demand™ kit were used for the genotyping. The SNPs of the NPTX2 gene were selected from the primer–probe list of Assays-on-Demand™ products for the ABI 7900HT to cover the full length of the gene. To increase statistical power, we selected the SNPs considering the minor allele frequencies indicated in the ABI primer–probe list and the HapMap public database. Four sets of primers and probes for SNPs with enough minor allele frequencies were available for our study. The db SNP IDs of the SNPs are shown in Table 1. These SNPs are located on the gene every 2.5–4.5 kb. According to the HapMap database, the SNPs which are located in the NPTX2 gene region form one or two haplotype blocks, including the 5′ and 3′ region, depending on race.

Statistical analyses were performed using the SAS/Genetics 9.1 software (SAS Institute Inc., Cary, North Carolina, USA). The frequencies of alleles and genotypes of each SNP were compared between patients and controls using the chi-square test. Subsequently, D' of the linkage disequilibrium between SNPs were analyzed. The frequencies of haplotypes consisting of SNPs, which were at a high linkage disequilibrium (haplotype block), were estimated. The exact p-values based on the likelihood ratio test with 10,000-permutation was calculated for comparison of the haplotype frequencies between patients and controls.

3. Results

The allele frequencies of the SNPs of the NPTX2 gene are summarized in Table 1. No significant difference was observed in genotypic distributions (not shown in the tables) or allele frequencies of the four markers of the NPTX2 gene between patients and controls. The minor allele frequencies of the SNPs were higher than 9% in all four SNPs. For all assayed SNPs, no significant departure from Hardy–Weinberg equilibrium was found.

The pair-wise D' values of the SNPs within the NPTX2 gene are summarized in Table 2. All four SNPs of the gene were in high linkage disequilibrium, forming a haplotype block. Regarding the pair-wise D' values, therefore, four marker haplotype of SNP1-4 (rs2291273, rs1681248, rs705318, rs705315), was tested.

Table 2
The strength of LD (denoted as D') between pairs of SNPs of NPTX2 in autism patients (lower diagonal) and controls (upper diagonal)

SNP	1	2	3	4
1		1.00	1.00	1.00
2	1.00		1.00	1.00
3	1.00	1.00		1.00
4	1.00	0.94	0.91	

Table 3
Estimated frequencies and permutation p-values for association of major NPTX2 haplotypes for rs2291273-rs1681248-rs705318-rs705315

Haplotype	Frequencies		Chi-square	p-value
	Case	Control		
C-G-G-G	0.51	0.52	0.06	0.81
C-G-T-G	0.20	0.20	0.03	0.85
C-C-T-A	0.18	0.18	0.04	0.85
T-G-G-G	0.08	0.09	0.11	0.76
C-G-T-A	0.01	0.01	0.14	0.69
Global p=0.39				

Haplotype frequencies were estimated >1%.

The estimated haplotype frequencies are shown in Table 3. No significant difference was observed in the estimated haplotype distributions between patients and controls.

4. Discussion

In this study, we genotyped four SNPs in the NPTX2 gene. Subsequently we compared estimated haplotype frequencies between autistic patients and normal controls in Japanese population. No evidence for association between the NPTX2 locus and autism was provided.

The 95% confidence intervals of the odds ratios were within 0.61 and 1.69 in all four SNPs of the gene. Assuming adequate statistical power to be >0.8, a sample size of 170 cases and 214 controls, and minor allele frequencies to be >0.1, our results might have adequate statistical power to contradict the effects of the gene with odds ratios of approximately 2.0 or more. However, sequencing in the patients may be necessary to evaluate a role of rare variants, which do not apply to a common disease common variant hypothesis.

In an analysis of the family history data of autism, Pickles et al. rejected single-locus and heterogeneity models in favor of a multilocus model that involves anything from two to ten loci (Pickles et al., 1995). If there were common or rare variants that brought functional alternations associated with autism, the variants would show linkage disequilibrium with the SNPs or haplotypes located near the variants. We thus investigated an association between the NPTX2 gene and autism, examining the presence of the association of the SNPs and haplotypes located in the region of the NPTX2 gene with autism. In this study, all four SNPs we investigated indicated high linkage disequilibrium with each other and, therefore, there would be a haplotype block covering all the NPTX2 gene domains in our sample.

The controls in this study were not age-matched to the patients. Twin and family studies indicate that autism might be highly heritable. The heritability estimate, calculated from the sibling recurrence risk and the MZ:DZ concordance ratio, is more than 90% (Bailey et al., 1995; Szatmari et al., 1998). Autism is a developmental disorder usually apparent by 3 years of age. In making a comparison between autistic patients and normal controls over 3 years of age, this lack of age-matching is not likely to have affected the results, considering the strong effect of genetic factors in autism compared with the rather

small effect of environmental factors (Folstein and Rosen-Sheidley, 2001). However, any variant that affects longevity may give spurious results when controls are not age-matched to patients in a genetic association study. This fact must be considered.

Another concern may be the population stratification of the sample, which could affect the results of studies in case–control design. This may not, however, significantly affect the present result, because the Japanese population is highly homogeneous, due to no major immigration for more than a thousand years, compared with the European or North American population. No subjects in this study had parents or grandparents of ethnicity other than Japanese.

In addition, the design of this study has limited statistical power that can exclude only major effects of the gene more than odds ratio 2.0 from the etiology of autism, and this design is based on a common disease common variants hypothesis. Further studies with larger sample size and sequencing of the NPTX2 gene are therefore needed to exclude a role of NPTX2 gene in autism.

5. Conclusion

In this report, we conducted a case–control study and haplotype analysis between the NPTX2 gene and autism. To our knowledge, no study has examined the role of NPTX2 variants in autism. While no association was observed in this study, considering the critical role of the gene in synapse formation and remodeling, further studies with larger samples or with family-based analyses may be recommended.

References

Bailey A, Le Couteur A, Gottesman I, Bolton P, Simonoff E, Yuzda E, et al. Autism as a strongly genetic disorder: evidence from a British twin study. Psychol Med 1995;25:63–77.

Carlsson ML. Hypothesis: is infantile autism a hypoglutamatergic disorder? Relevance of glutamate — serotonin interactions for pharmacotherapy. J Neural Transm 1998;105:525–35.

Dodds DC, Omeis IA, Cushman SJ, Helms JA, Perin MS. Neuronal pentraxin receptor, a novel putative integral membrane pentraxin that interacts with neuronal pentraxin 1 and 2 and taipoxin-associated calcium-binding protein 49. J Biol Chem 1997;272:21488–94.

Folstein SE, Rosen-Sheidley B. Genetics of autism: complex aetiology for a heterogeneous disorder. Nat Rev Genet 2001;2:943–55.

Hollmann M, Heinemann S. Cloned glutamate receptors. Annu Rev Neurosci 1994;17:31–108.

Hsu YC, Perin MS. Human neuronal pentraxin II (NPTX2): conservation, genomic structure, and chromosomal localization. Genomics 1995;28:220–7.

Izutsu T, Osada H, Tachimori H, Naganuma Y, Kato S, Kurita H. The usefulness of the child behavior questionnaire revised (CBQ-R) as a supplementary scale for diagnosis of pervasive developmental disorders. Rinsyo-Seishin Igaku 2001;30:525–32.

Kirkpatrick LL, Matzuk MM, Dodds DC, Perin MS. Biochemical interactions of the neuronal pentraxins. Neuronal pentraxin (NP) receptor binds to taipoxin and taipoxin-associated calcium-binding protein 49 via NP1 and NP2. J Biol Chem 2000;275:17786–92.

O'Brien RJ, Xu D, Petralia RS, Steward O, Huganir RL, Worley P. Synaptic clustering of AMPA receptors by the extracellular immediate-early gene product Narp. Neuron 1999;23:309–23.

Pickles A, Bolton P, Macdonald H, Bailey A, Le Couteur A, Sim CH, et al. Latent-class analysis of recurrence risks for complex phenotypes with selection and measurement error: a twin and family history study of autism. Am J Hum Genet 1995;57:717–26.

Risch N, Spiker D, Lotspeich L, Nouri N, Hinds D, Hallmayer J, et al. A genomic screen of autism: evidence for a multilocus etiology. Am J Hum Genet 1999;65:493–507.

Steffenburg S, Gillberg C, Hellgren L, Andersson L, Gillberg IC, Jakobsson G, et al. A twin study of autism in Denmark, Finland, Iceland, Norway and Sweden. J Child Psychol Psychiatry 1989;30:405–16.

Szatmari P, Jones MB, Zwaigenbaum L, MacLean JE. Genetics of autism: overview and new directions. J Autism Dev Disord 1998;28:351–68.

Tsui CC, Copeland NG, Gilbert DJ, Jenkins NA, Barnes C, Worley PF. Narp, a novel member of the pentraxin family, promotes neurite outgrowth and is dynamically regulated by neuronal activity. J Neurosci 1996;16:2463–78.

ELSEVIER

Clinical Neurophysiology 118 (2007) 1464–1471

www.elsevier.com/locate/clinph

Electrophysiological abnormalities of spatial attention in adults with autism during the gap overlap task

Yuki Kawakubo [a,*], Kiyoto Kasai [a], Shinji Okazaki [b], Miyuki Hosokawa-Kakurai [c], Kei-ichiro Watanabe [d], Hitoshi Kuwabara [a], Michiko Ishijima [a], Hidenori Yamasue [a], Akira Iwanami [e], Nobumasa Kato [f], Hisao Maekawa [b]

[a] *Department of Neuropsychiatry, Graduate School of Medicine, University of Tokyo, 7-3-1 Hongo, Bunkyo-ku, Tokyo 113-8655, Japan*
[b] *Institute of Disability Sciences, University of Tsukuba, Tsukuba 305-8572, Japan*
[c] *Faculty of Education and Care of Early Childhood, Fuji Tokoha University, Fuji 417-0801, Japan*
[d] *Department of Child Psychiatry, School of Medicine, University of Tokyo, Tokyo 113-8655, Japan*
[e] *Department of Neuropsychiatry, Saitama Medical University, Iruma 350-0495, Japan*
[f] *Department of Psychiatry, School of Medicine, Showa University, Tokyo 142-8555, Japan*

Accepted 14 April 2007

Abstract

Objective: We evaluated event-related potentials (ERPs) elicited by attentional disengagement in individuals with autism.
Methods: Sixteen adults with autism, 17 adults with mental retardation and 14 healthy adults participated in this study. We recorded the pre-saccade positive ERPs during the gap overlap task under which a peripheral stimulus was presented subsequent to a stimulus in the central visual field. Under the overlap condition, the central stimulus remained during the presentation of the peripheral stimulus and therefore participants need to disengage their attention intentionally in order to execute the saccade to the peripheral stimulus due to the preservation of the central stimulus.
Results: The autism group elicited significantly higher pre-saccadic positivity during a period of 100–70 ms prior to the saccade onset than the other groups only underthe overlap condition. The higher amplitude of pre-saccadic positivity in the overlap condition was significantly correlated with more severe clinical symptoms within the autism group.
Conclusions: These results demonstrate electrophysiological abnormalities of disengagement during visuospatial attention in adults with autism which cannot be attributed to their IQs.
Significance: We suggest that adults with autism have deficits in attentional disengagement and the physiological substrates underlying deficits in autism and mental retardation are different.

Keywords: Autism; Spatial attention; Event-related potentials; Saccadic eye movement

1. Introduction

Autism is diagnosed on the basis of behavioral and developmental features such as impairment of reciprocal social interaction, communication and imagination, and the presence of repetitive and ritualistic behavior. It has been recently pointed out that scientific merits from studies using a comprehensive model assuming a single explanation for autism may be limited, since various behavioral features of autism are largely independent in terms of genetic background as shown by twin cohort studies (Happé et al., 2006). Thus, a bottom-up type approach which explores abnormal or preserved functions in relatively fundamental cognitive processes based on simple cognitive models may be important in the autism research strategy. Researchers have proposed that attentional abnormalities underlie the behavioral features of autism such as inflexibility, repetitive

* Corresponding author. Tel.: +81 3 5800 9263; fax: +81 3 5800 6894.
E-mail address: yukik-tky@umin.ac.jp (Y. Kawakubo).

1388-2457/$32.00
doi:10.1016/j.clinph.2007.04.015

behavior and overselectivity (Lovaas et al., 1979; Casey et al., 1993; Townsend et al., 1996, 2001; Wainwright and Bryson, 1996; Senju et al., 2004). Auditory attention has been intensively studied in the literature, particularly using event-related potentials (ERPs). For example, a reduced P300 amplitude (Oades et al., 1988; Lincoln et al., 1993) and abnormal mismatch negativity (Gomot et al., 2002; Kasai et al., 2005) have been reported. On the other hand, spatial attention has been also implicated in the pathophysiology of autism, which has been understudied.

Spatial attention is a function of spatially directed attention and spatial selectivity (Allport, 1989). Posner and Cohen (1984) outlined a model in which the successive components of spatial attention were defined as disengagement, shift, and engagement of attentional sources. In Posner's cuing paradigm, a target stimulus follows a cue stimulus presented on the same side of a target (valid condition) or on the contralateral side of a target (invalid condition). This task makes it possible to investigate the ability to disengage attention from one location and shift attention to its contralateral location. Findings from patients with acquired brain damage suggest that these components are associated with specific brain areas, i.e., disengagement is associated with the parietal cortex, shift is related with superior colliculus, and engagement is associated with thalamus (Posner and Cohen, 1984; Posner and Petersen, 1990).

Most studies on visuospatial attention in adults with autism have used the cuing paradigm that elicits the reorienting of the direction of the attention (Posner, 1980) and reported behavioral problems in attentional disengagement and shift (Casey et al., 1993; Townsend et al., 1996, 2001; Wainwright and Bryson, 1996), but findings of other studies using eye gaze cue have been mixed (Senju et al., 2004; Swettenham et al., 2003; Kylliäinen and Hietanen, 2004). Other studies reported that autistic children presented the difficulties disengaging attention from the salient object (Hughes and Russell, 1993) and mental concepts (Hughes et al., 1994). On the other hand, studies using the gap paradigm (Saslow, 1967) have shown impairment of attentional engagement in children (van der Geest et al., 2001) and adults (Kawakubo et al., 2004) with autism. In the gap overlap task, when a temporal gap is introduced between the disappearance of a central fixation point and the appearance of a new target stimulus, the saccade reaction times are reduced compared to when no gap is introduced (gap effect; Saslow, 1967). This difference in saccade reaction times has been explained by the difference in attentional disengagement(Fischer and Weber, 1993). In the gap condition, in which an initial fixation point disappears before a target appears, attention on the fixation point is disengaged automatically. On the other hand, in the overlap condition, in which the fixation point remains after the target appears, attention on the fixation point is disengaged due to the appearance of the peripheral target stimulus. Therefore, the saccade reaction times in the overlap condition are longer than in the gap condition. It cannot be concluded, however, that individuals with autism show only impairment of attentional engagement but not of disengagement in the gap paradigm. If the engaging of attention to the central fixation point is enhanced, they may show impairment of attentional *disengagement*. In order to clarify whether individuals with autism have an impairment of attentional disengagement in the gap paradigm, further examination under conditions in which attentional engagement to the central visual field is ensured is necessary.

Moreover, little is known of the *physiological* substrates for these visuospatial attentional deficits in autism. In the visual ERP literature, P300 amplitude of individuals with autism under a condition where the target stimulus was presented in the center of visual field was comparable to that of normal controls (Pritchard et al., 1987; Ciesielski et al., 1990). On the other hand, when the stimulus was presented at various peripheral locations individuals with autism were associated with smaller-than-normal visual P300 amplitude (Kemner et al., 1999; Townsend et al., 2001). To our knowledge, however, no previous studies have directly examined ERPs elicited by attention disengagement in individuals with autism.

Csibra et al. (1997) and Gómez et al. (1996) analyzed saccade-locked ERP during the gap/overlap task in *healthy* adults, and found a slowly developing pre-saccadic positivity elicited at central–parietal electrode sites that was followed by a pre-saccadic spike potential immediately preceding the eye movement. Csibra et al. (1997) concluded that attentional disengagement in the gap overlap task was reflected in these parietal positive ERP components.

Thus, the goal of this study was to assess the pre-saccade positive ERP components during the gap overlap task as an electrophysiological index of attentional disengagement in adults with autism. To ensure attentional engagement to the central visual field, our task was different from a typical format of the gap overlap task in some points that various pictures were used as stimuli instead of a cross and a square and participants were required to discriminate the stimuli. Moreover, to clarify whether the physiological dysfunction of visuospatial attention was specific to autism rather than being attributable to general intellectual disability, we compared the data from adults with autism with those of IQ-matched adults with mental retardation. Previous studies (Csibra et al., 1997; Gómez et al., 1996) indicated that the pre-saccadic positivity was higher in the overlap condition than in the gap condition. Thus, it is assumed that the pre-saccadic positivity reflects the resource that is needed to disengage the attention. Accordingly, we hypothesized that the autistic group would exhibit impairment in attentional disengagement under the overlap condition that would be reflected as higher or longer pre-saccadic positivity detected in the saccade-locked ERPs. Moreover, we predicted higher pre-saccadic positivity would be associated with severer autistic symptoms.

2. Method

2.1. Participants

Sixteen adults with autism (11 men and 5 women; mean age [SD], 29.0 [6.5]; mean IQ [SD], 43.6 [14.7]), 17 adults with mental retardation (12 men and 5 women; mean age [SD], 27.5 [5.0]; mean IQ [SD], 40.6 [10.9]), and 14 healthy adults (6 men and 8 women; mean age [SD], 28.5 [5.8]; mean IQ [SD], 105.2 [10.9]) participated in this study. Age (one-way ANOVA, $p = 0.70$) and gender (χ^2 test, $p = 0.23$) were not significantly different among groups. IQs were evaluated with the Wechsler Adult Intelligence Scale-Revises (WAIS-R) for two of autism participants and with the Tanaka-Binet Test for eleven of autism participants and all individuals with mental retardation. For healthy adults IQs were estimated by four subtests of the WAIS-R. Autism subjects and mentally-retarded subjects did not significantly differ in IQ (t-test, $p = 0.52$). Diagnosis of autism was determined according to DSM-IV criteria and Childhood Autism Rating Scale (CARS: Schopler et al., 1988) by a trained pediatric psychiatrist (clinical experience >5 years; KW, HK, or MI). We used a CARS score of 27 as the cutoff point (Mesibov et al., 1989). Autism subjects had significantly higher CARS scores than mentally-retarded subjects (34.1 [SD = 4.1] versus 20.3 [3.1]; t-test, $p < 0.001$). All participants had normal or corrected to normal vision and did not have any chromosomal or neurological disorders. All participants were right-handed determined using the Edinburgh Inventory. The Ethical Committee of the Faculty of Medicine, University of Tokyo, approved this study (No. 629). Written informed consent was obtained from all participants and their parents before the experiment.

2.2. Stimuli and apparatus

The stimuli were presented on a 21-in. CRT display with a black background by using STIM software (Neuroscan, Inc.). To encourage the motivation of the participants, we used as stimuli 13 illustrations that consisted of pictures of animals (e.g., dog, frog), daily goods (e.g., glasses, baggage) and vehicles (e.g., bicycle, car), etc. In place of a fixation point a central stimulus (picture stimulus as above) was presented in the central visual field. Peripheral stimuli were presented 14 degrees (deg.) to the left or right of the central stimulus. All stimuli were of the same angular size; 1.3 × 1.3 deg (Fig. 1).

2.3. Procedure

Participants were seated 0.60 m away from the CRT monitor with their chin on a chinrest. Participants initiated each trial by pressing a start button, and after 1000 ms a central stimulus was presented in the center of the CRT monitor. A peripheral stimulus was then presented to the left or right side of the central stimulus for 2000 ms. To minimize the possibility that participants anticipate the timing of the peripheral stimulus onset, the central stimulus was presented at intervals randomly varying between 700 and 1500 ms. To make the task clearer to participants, we instructed them to press a button when a target stimulus, the drawing of a dog, appeared as either the central stimulus or the peripheral stimulus. In some trials, the dog was presented both in the center and he peripheral visual field. Thus, even if the dog was presented in the center, saccades were required. Since it was difficult to ask button pressing at an appropriate timing for three subjects, these subjects were alternatively asked to speak aloud the name of the target stimulus. It was necessary for participants to move their eyes to the peripheral stimulus when it was presented, in order to discriminate the target stimulus from the other stimuli.

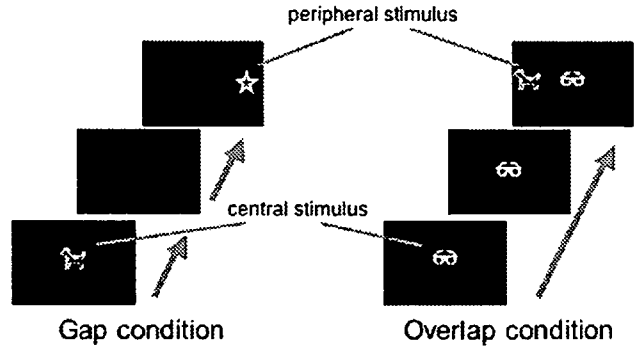

Fig. 1. Experimental procedures in the gap condition (left) and the overlap condition (right). In the gap condition, the central stimulus disappeared 200 ms before the peripheral stimulus was presented, and in the overlap condition, the central stimulus remained during the presentation of the peripheral stimulus. The participants were instructed to press a button when a target stimulus, the drawing of a dog, appeared as either the central stimulus or the peripheral stimulus.

In the gap condition, the central stimulus disappeared 200 ms before the peripheral stimulus was presented, and in the overlap condition, the central stimulus remained during the presentation of the peripheral stimulus. Practice trials were given to each participant to ensure that the instructions had been understood. After the practice trials, 180 trials composed of 45 trials of each of the four conditions ([Gap vs. overlap] × [left- vs. right-side presentation on the monitor]) were presented in a random order in three blocks of 60 trials each. The probability of the appearance of target stimulus was 20%.

2.4. Recordings

The scalp electroencephalogram (EEG) was recorded according to the international 10–20 system using Ag/AgCl electrode caps (Neuroscan, Inc.) at 16 electrode sites (F3, Fz, F4, T3, C3, Cz, C4, T4, T5, P3, Pz, P4, T6, O1, Oz, O2) referred to linked earlobes. The horizontal electrooculogram (EOG) was recorded at the outer canthi of the both eyes and the vertical EOG was recorded from electrodes

placed below and above the left eye. The bandpass filter was set at 0.15–30 Hz and the sampling rate was 500 Hz. EEGs and EOGs were analyzed using SCAN system with SynAmps (Neuroscan, Inc.).

2.5. Data analysis

A saccade was defined as the first moment at which the velocity of the eye exceeded 22 deg/sec. Trials were excluded from further analysis if: (1) the target stimulus was presented in that trial, (2) the eyes moved before the peripheral stimulus onset, and (3) the saccade occurred in the incorrect direction or saccadic reaction times (SRTs) were less than 80 ms. Express saccade was defined as saccade that occurred between 80 and 130 ms after the presentation of the peripheral stimulus (Fischer and Weber, 1993). Trials with EEG range exceeding 100 μV at any EEG electrode were rejected as artifact. We used the 50-ms period starting 150 ms before the saccade onset as the baseline as no salient activities at any electrode in this period. The four conditions (i.e., [Gap vs. overlap] × [left- vs. right-side presentation on the monitor]) were averaged separately. The mean number of accepted sweeps was above 20 for all conditions and for all groups, and did not significantly differ between conditions or between groups. Pre-saccadic positivity was defined as a slowly developing positivity 100 ms before the saccade onset, and the pre-saccadic spike potential was defined as a sharp positivity peaking immediately before the saccade onset.

For the group comparison of the SRT, repeated measures ANOVA was performed with the group (autism, mental retardation, control) as the between-subject factor, and the condition (gap, overlap) and the presentation side (left, right) as within-subject factors. For all repeated measures ANOVAs, the sphericity assumption was tested using Mauchley's test, and Greenhouse-Geisser correction was performed when there was a significant violation of the sphericity assumption. Tukey's honestly significant difference test was used for post hoc multiple comparisons.

To compare the time course of the pre-saccadic positivity, the averaged amplitude was calculated within 30 ms windows from 100 to 70 ms and from 70 to 40 ms before the saccade onset. Then repeated measures ANOVA was performed for each of the pre-saccadic positivity amplitude (averaged across 30 ms), with the group as between-subject factor and the condition, the side of presentation and the electrode (C3, Cz, C4, P3, Pz, P4, O1, Oz, O2) as the within-subject factors. In order to determine the latency of pre-saccadic spike potential, the computation of global field power (GFP: Lehmann and Skrandies, 1980) was applied to the waveform for each subject and condition. The individual pre-saccadic spike potential amplitudes were determined as the amplitude at the GFP peak latency. Repeated measures ANOVA was performed to compare the pre-saccadic spike potential amplitudes with the group as between-subject factor and the condition, the side of presentation and the electrode as the within-subject factors.

Spearman's rank-correlation coefficient was used in exploratory analyses of the relationships between SRT and scores on each item of the CARS and IQ, and between pre-saccadic positivity amplitudes (averaged amplitudes over nine electrodes for both sides of presentation under each condition) at −100 to −70 ms and −70 to −40 ms periods, where the pre-saccadic positivity amplitudes showed significant group differences, and scores on each item of the CARS and IQ. The level for significance was not corrected for multiple comparisons due to the preliminary nature of the correlational analyses.

3. Results

3.1. Behavioral data

In this study, individuals with autism did not show more frequent express saccade than the other two groups either in the gap or overlap condition; the express saccade rate under the gap condition was larger than that under the overlap condition in all three groups (autism group; $z = 2.10$, $p < 0.05$, MR group; $z = -3.62$, $p < 0.001$, healthy control group; $z = -3.23$, $p < 0.01$).

The repeated measures ANOVA of the SRT data showed a significant main effect of Condition ($F[1,44] = 45.7$, $p < 0.001$) and Group ($F[2,44] = 4.36$, $p = 0.019$), and a significant Group × Condition interaction ($F[2,44] = 4.29$, $p = 0.02$) (Fig. 2). No significant main effect of the side of presentation or other interactions was found (Table 1). We thus performed a one-way ANOVA for each condition after data for both sides of the presentation were averaged. The main effect of group was significant in the overlap condition ($F[2,44] = 4.71$, $p = 0.014$) but not in the gap condition ($F[2,44] = 2.86$, $p = 0.068$). The multiple comparison test under the overlap condition revealed that the autism group showed significantly longer SRTs than the control group ($p = 0.01$), while the mental retardation group was not significantly different in SRTs from either group (p's = 0.15, 0.45, respectively).

Mean correct response to the target stimuli (discrimination of the dog) was 63% in the autism group, 68% in the MR group and 98% in the healthy control group, respectively. Thus, although autism and MR groups performed

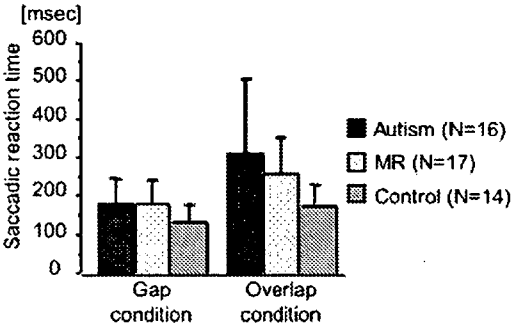

Fig. 2. Saccadic reaction times for the autism group (Autism), the mental retardation group (MR) and the control group (Control).

Table 1
Results of the repeated measures ANOVA of the SRT

	df	F	p
Main effects			
Group	2	4.364	**0.019***
Condition	1	45.74	**<0.001*****
Side of presentation	1	0.062	0.805
Interactions			
Group Â~ Condition	2	4.289	**0.02***
Side of presentation Â~ Group	2	0.883	0.421
Side of presentation Â~ Condition	1	0.022	0.882
Side of presentation Â~ Condition Â~ Group	2	0.363	0.697

Bold values show significant differences.
* $p = 0.05$.
*** $p = 0.001$.

worse than the control group, these groups were able to understand the task procedure. Additionally, t-test for the correct response between the MR group and the autism group did not show significant difference ($t[1,26] = 0.432$, $p = 0.67$).

3.2. Pre-saccadic positivity

Visual inspection of the ERP waveforms and topographic mappings indicated that pre-saccadic positivity increased around 100 and 40 ms prior to the saccade onset under the overlap condition in the autism group (Figs. 3–5). The ANOVA of the pre-saccadic positivity amplitude for the 100–70 ms before the saccade onset showed a significant Condition × Side × Group interaction ($F[2,44] = 3.52$, $p = 0.038$) and a significant main effect of Group ($F[2,44] = 3.86$, $p = 0.029$). No other significant interactions were found. After the amplitudes at all electrodes were averaged, two-way ANOVA was performed separately for each condition. Under the gap condition, no significant main effect of Group ($F[2,44] = 0.43$, $p = 0.65$) or interaction of Side × Group ($F[2,44] = 0.834$, $p = 0.44$) was found.

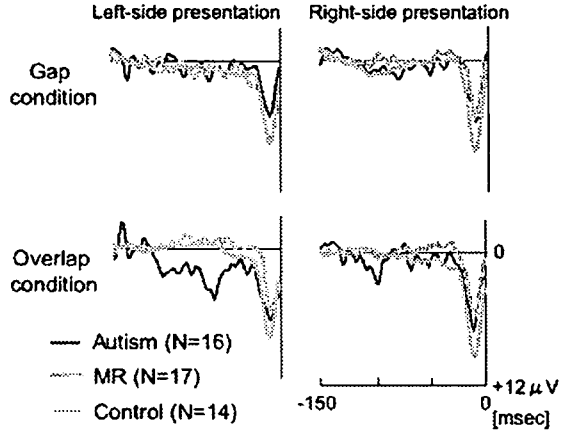

Fig. 3. Grand-averaged waveforms at Pz in the gap condition (top) and the overlap condition (bottom). Black lines are for the autism group, dot lines are for the mental retardation group, and gray lines are for the control group.

On the other hand, under the overlap condition, there was a significant main effect of Group ($F[2,44] = 5.47$, $p = 0.008$) but there was no significant interaction of Side × Group ($F[2,44] = 1.64$, $p = 0.21$). Multiple comparisons found that the autism group elicited higher pre-saccadic positivity than both mental retardation ($p = 0.011$) and control ($p = 0.029$) groups in the overlap condition.

In the ANOVA of the pre-saccadic positivity amplitude for the 70–40 ms, there was a significant interaction of Condition × Electrode × Group ($F[16,352] = 2.89$, $p = 0.018$, $\epsilon = 0.31$) and significant main effect of Group ($F[2,44] = 3.89$, $p = 0.028$). However, there were no other significant interactions. After the amplitudes for both sides of presentation were collapsed, two-way ANOVA was performed for each condition. Under the gap condition, no significant main effect of Group was found ($F[2,44] = 0.40$, $p = 0.67$) but there was a significant interaction of Electrode × Group ($F[16,352] = 6.36$, $p < 0.0001$). The post hoc analysis for the electrode in the gap condition indicated that, at O2 and Oz, the autism group elicited higher pre-saccadic positivity than the mental retardation group (O2: $p = 0.009$; Oz: $p = 0.035$). Under the overlap condition, there was no significant group × electrode interaction ($F[16,352] = 0.96$, $p = 0.45$) but there was a significant main effect of Group ($F[2,44] = 5.63$, $p = 0.007$). The multiple comparison test under the overlap condition showed that pre-saccadic positivity in the autism group was higher than that in the mental retardation group ($p = 0.005$).

3.3. Pre-saccadic spike potential

Pre-saccadic spike potentials that peaked 10 ms prior to the saccade onset were observed at broad centro-parietal sites in all groups and conditions (Figs. 3 and 4). For the pre-saccadic spike potential amplitude, the ANOVA showed a significant interaction of Electrode × Group ($F[16,352] = 3.94$, $p = 0.001$, $\epsilon = 0.44$). However, the follow-up analysis for each electrode showed no significant group difference ($F[2,44] = 0.37$–2.78, $p = 0.073$–0.77). These results suggest that there was no group difference for pre-saccadic spike potential.

3.4. Correlations with the clinical data

SRTs were not significantly correlated with IQs or scores on each item of the CARS. There were significant correlations between pre-saccadic positivity amplitude for 100–70 ms under the overlap condition and two items of CARS (Imitation: $r = 0.53$, $p = 0.041$; Near receptor responsiveness: $r = 0.55$, $p = 0.034$).

4. Discussion

To our knowledge, this is the first study that provides electrophysiological evidence for dysfunction of attentional disengagement indexed by saccade-locked ERPs in individuals with autism. We speculate that the higher pre-saccadic